

# Carbon Nitrides in Photoelectrochemistry: State of the Art and Perspectives Beyond Water Splitting

Sirlon F. Blaskievicz,\* Juliana Lucca Francisco, Frank Marken, and Lucia Helena Mascaro

Cite This: <https://doi.org/10.1021/acsaem.3c02623>

Read Online

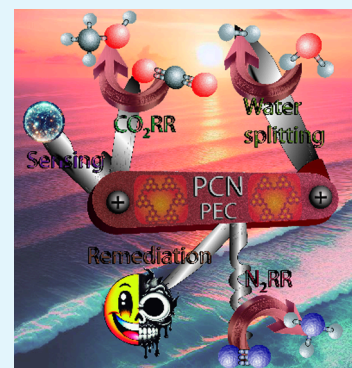
ACCESS |

Metrics &amp; More

Article Recommendations

**ABSTRACT:** Photoelectrodes made from cost-effective materials are the most desired for practical photoelectrochemical (PEC) applications, aiming to help in the imminent environmental crisis that urges an energetic transition. A prominent class of semiconductors are the polymeric carbon nitrides (PCN), which appear to be an eco-friendly solution particularly for green hydrogen production through water splitting, value-added organic compounds obtention from biomass upgrading, or CO<sub>2</sub> reduction; even green ammonia can be obtained by PEC reduction of N<sub>2</sub>. In this sense, monitoring dangerous environmental species or converting them into less toxic ones can also be performed through PEC using carbon nitride-based electrodes. In this review, we provide an overview of the basics of PCN applications in PEC, including commonly employed strategies to enhance their performance. Additionally, we discuss the current state-of-the-art for PCN in PEC water splitting as well as lesser-explored areas such as biomass upgrading, environmental remediation, photoelectroanalytical sensing, and light-driven CO<sub>2</sub> and N<sub>2</sub> reduction reactions. Finally, we present an overview of prospects for PCN material in PEC.

**KEYWORDS:** hydrogen evolution, biomass oxidation, CO<sub>2</sub> reduction, N<sub>2</sub> reduction, PEC sensing



## 1. INTRODUCTION

In the coming decades, energy transition and environmental problems will be major challenges faced by contemporary society.<sup>1</sup> To address the looming crisis and limit environmental pollution, developing photoelectrochemical technologies that use natural solar radiation as a parcel of energy input can reduce the costs and be an important tool for the green production of fuels and value-added chemicals, as well as to monitor and detoxify environmentally hazardous species. In this sense, cost-effectively and sustainably, it is preferable to avoid the usage of costly and/or toxic chemical elements while considering cost, scalability, and environmental impact. Certain semiconductors based on inorganic oxides, like TiO<sub>2</sub> fit in some of the above-presented characteristics, once they have good chemical stability, guarantee long-term operations,<sup>2,3</sup> and present low toxicity.<sup>4</sup> What leads to hindrance in the practical employment of pristine TiO<sub>2</sub> for photoelectrochemistry (PEC) is their large bandgap ( $E_g$ ), comprehending the UV range, which turns into low utilization of the natural solar spectra<sup>5–8</sup> and therefore resulting in photoresponses that fall short of theoretical limits.<sup>9,10</sup> Apart from the oxides, the cadmium chalcogenides (e.g., CdS, CdSe, and CdTe) represent a well-studied class of semiconductors, regarded as good candidates for better natural radiation utilization, due to their  $E_g$  ranging from ~2.4 to 1.5 eV, covering the visible and near-infrared spectrum.<sup>4,11</sup> However, the applicability of these chalcogenides is also limited due to

cadmium being a scarce element in the earth's crust,<sup>12</sup> and mainly by characteristics not desirable from the point of view of green chemistry: its high toxicity to both human health<sup>13</sup> and the environment.<sup>4</sup>

When low-toxicity alternatives to cadmium chalcogenides are sought, carbon nitrides can be considered as a hotspot. Pumera and co-workers evaluated the toxicity of two kinds of carbon nitrides (triazine and heptazine types), identifying a dose-dependent toxicological effect on human lung carcinoma epithelial cells (A549).<sup>14</sup> The triazine-based material was found to be more cytotoxic than the heptazine-based material, which was attributed to the different N/C ratios. In comparison to analogous materials like graphene oxide,<sup>15</sup> however, the toxicity was much lower.

Carbon nitrides (C<sub>3</sub>N<sub>4</sub>) comprise a class of 2D materials that have a layered structure similar to graphene,<sup>16,17</sup> composed of carbon and nitrogen atoms arranged in a hexagonal lattice, with alternating single and double bonds between the atoms forming triazine or tri-s-triazine (heptazine) rings, as shown in Figure 1. In comparison to some of the

**Received:** October 18, 2023

**Revised:** March 14, 2024

**Accepted:** March 18, 2024

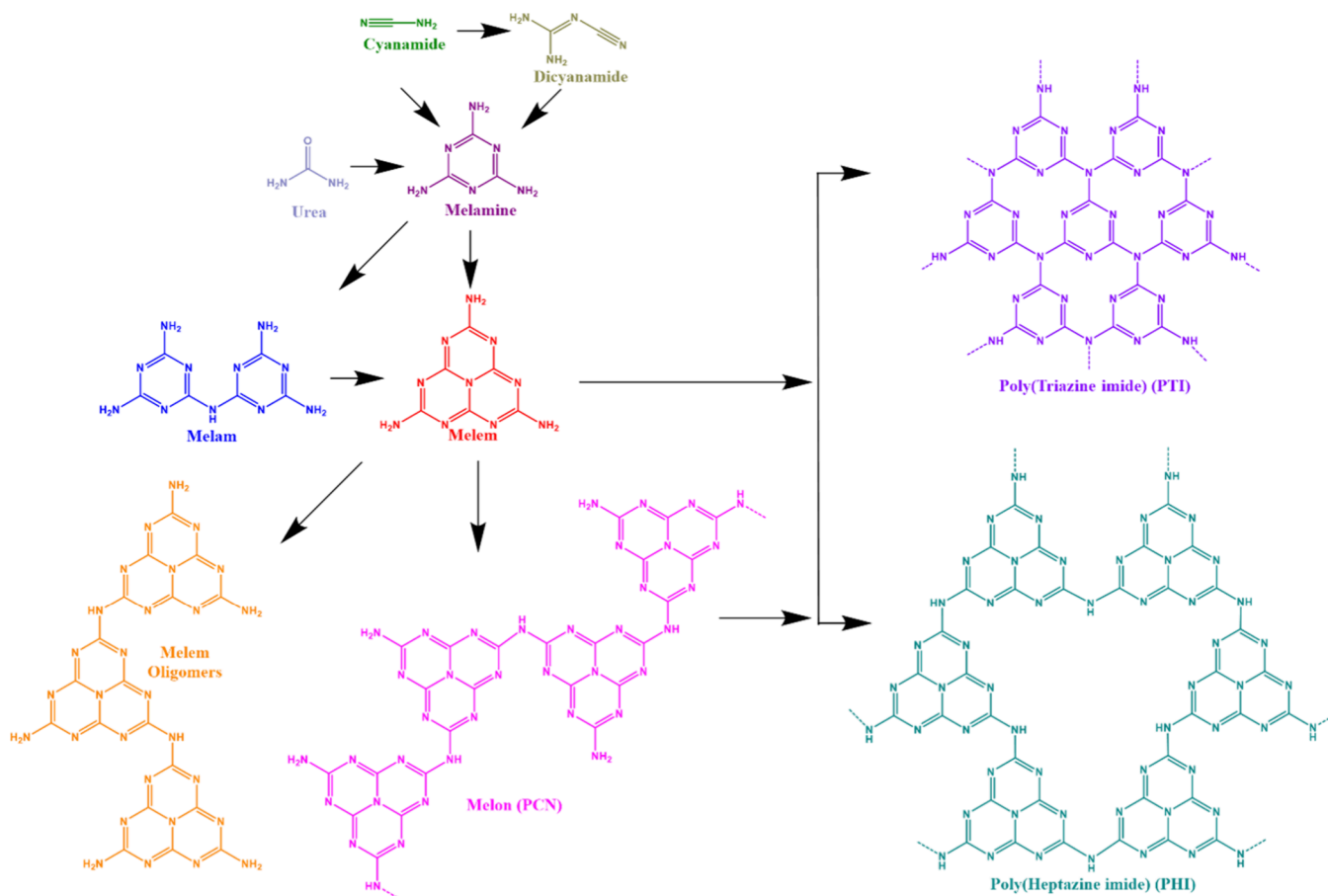


**Figure 1.** Representation of some synthetic paths that lead to the structures of the polymeric carbon nitrides from the types melon (PCN), poly(triazine imide) (PTI), and poly(heptazine imide) PHI.

traditional inorganic semiconductors,  $\text{C}_3\text{N}_4$  possesses a similar range of light harvesting, generally around 500 nm,<sup>18,19</sup> the alternated double and single bonds in its structure make this a very robust class of material, granting it a good chemical and thermal stability.<sup>20–22</sup> Anyhow, both the optical and physical properties of carbon nitrides can be easily modulated according to different synthetic methods or later modifications that will be discussed in this review.

Usually, in the literature, the name “graphitic” carbon nitride ( $\text{g-C}_3\text{N}_4$ ) is used due to the initial characterization of this material, where a peak equivalent to the  $\pi$ - $\pi$  stacking of graphite was observed. However, later it was reported to appear in any plane and aromatic molecule like naphthalene.<sup>23</sup> Moreover, this denomination is considered incorrect because a “purely” graphitic carbon nitride represents a structure formed only by carbon and nitrogen atoms, with tertiary amines connecting the bases triazines or heptazines moieties. The polymeric carbon nitride (PCN) structures, synthesized by thermal polymerization of nitrogen-containing precursors like cyanamide,<sup>24,25</sup> dicyanamide,<sup>26–28</sup> urea,<sup>29–32</sup> and melamine,<sup>33–35</sup> among others,<sup>36,37</sup> are obtained as amorphous or crystalline structures.

The synthesis methods regarding temperature and precursors employed have a direct influence on modulating the final properties of the obtained carbon nitride, such as light absorption,  $E_g$  band position, charge separation efficiency, and surface area, which in turn on the possible applications for the PCN. Schwarzer et al. discussed that the ideal thermopolyme-

rization temperature takes place at temperatures in the range of 450–650 °C.<sup>38</sup> Below this range, the polymerization is incomplete, while above, the PCN materials start to degrade. Additionally, changing the precursor from urea to thiourea allows changing the PCN band gap from up to 2.78 to ca. 2.58 eV.<sup>39</sup> On the other hand, controlled atmospheres during the heat treatment step can lead to structural alterations, as seen in the work of Niu et al., where heating in a hydrogen atmosphere generated a PCN with nitrogen vacancies. The material obtained showed a photocatalytic performance superior to an unmodified nitride and a reduced band gap of 2.03 eV.<sup>40</sup>

The  $\text{C}_3\text{N}_4$  materials can be divided into two main classes: the “conventional” type, which is obtained by the direct pyrolysis of CN-containing compounds, as mentioned above, resulting in melon structures (named henceforth as PCN) (Figure 1); the second type is the “ionic” carbon nitrides, which in the case of a highly controlled polymerization to generate materials with higher crystallinity and with well-defined “building blocks”, *i.e.*, basic units that constitute the polymer as represented in Figure 1, give rise to poly(triazine imide) (PTI) and poly(heptazine imide) (PHI).

For obtaining ionic carbon nitrides, the primary method identified in the literature is the pyrolysis of the nitrogen precursor in a medium with eutectic mixtures of salts,<sup>41–43</sup> the presence of salts containing alkali metals such as Na, K, and Li results in negatively charged pyridinic nitrogen in the structure, thereby balancing the charge of the alkali ion. In addition, an ion exchange process allows replacing the alkali ions by the

coordination of ions of a given transition metal M, generating a platform for single atom catalysts.<sup>44</sup> The ionic carbon nitrides are thus highly organized, and the interaction between the organic precursor and condensation intermediates with the ions present in the salt employed is critical to the type of nitride generated, as demonstrated in the work of Antonietti et al.<sup>45</sup> By using melamine and NaCl, the authors obtained PHI, while PTI was obtained when using LiCl. One difference observed in the properties of more organized and crystalline materials is in their conductivity, wider and more organized sheets increase the diffusion path of photogenerated charge carriers, decreasing the recombination of the  $e^-/h^+$  pairs, and consequently leading to better catalytic performance.<sup>23,46,47</sup> In addition, ionic carbon nitrides present unique properties not observed in conventional PCNs, such as accumulating and storing light in the form of long-lived radicals for posterior use, in a process named “dark” photocatalysis,<sup>48</sup> or in photodoping that leads to a significant improvement of the photoresponse.<sup>49</sup>

Considered a rising star in photo and photoelectrochemistry for the last decades, there are plenty of works employing this class of materials for environmental remediation in both photo,<sup>50–52</sup> and photoelectrocatalysis.<sup>53</sup> Since their potential as a catalyst for hydrogen evolution from aqueous media was demonstrated in 2008,<sup>54</sup> a wide range of research has been directed toward improving the photoactivity efficiency of PCNs with remarkable advances in the area of photoelectrochemistry (PEC). The main focus of work with carbon nitride is still hydrogen production, demonstrated by the number of publications in the last 10 years (Figure 2),

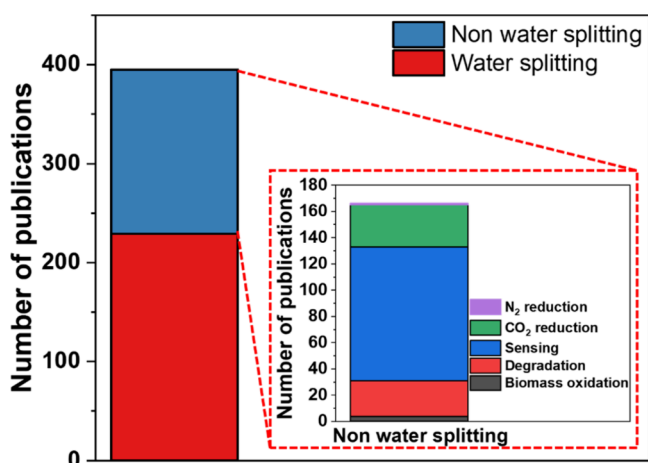


**Figure 2.** Number of reports in indexed journals concerning photoelectrochemical applications of carbon nitrides from 2014 to 2024. The data were obtained from the Scopus platform in March of 2024 using a combined search of the following keywords: “carbon nitride”; “photoelectrochemical”; “photoelectrochemistry”; “water splitting”; “biomass”; “degradation”; “sensor”; “CO<sub>2</sub> reduction”; and “N<sub>2</sub> reduction”.

primarily via water splitting.<sup>55–57</sup> However, the versatility of polymeric carbon nitrides is highlighted by the plethora of themes they encompass, including biomass upgrading, pollutant degradation, and sensing, as well as the reduction of atmospheric nitrogen and carbon dioxide.

In this review, we aim to explore recent advances in the design and synthesis of polymeric carbon nitride materials for photoelectrocatalytic applications, including synthetic pathways for preparing various PCNs on different substrates,

modifications, and combinations with other materials. We discuss limitations that currently hinder their use in PEC devices. Additionally, will present PEC applications of PCNs in hydrogen generation from water splitting, N<sub>2</sub>, and CO<sub>2</sub> reduction, environmental remediation, and sensing. Lastly, this review provides insights into the challenges and future directions for the application of polymeric carbon nitride photocatalysts in society.

## 2. STRATEGIES TO ENHANCE CARBON NITRIDE PHOTOELECTROCHEMICAL PERFORMANCE

To be feasible, photoredox reactions rely on three primary processes: (i) light absorption/harvesting; (ii) charge carrier generation/separation; and (iii) surface electron/hole transfer and recombination reactions. As the overall performance is determined by the balance between these three steps, the application of an external bias as occurs on PEC can improve steps (ii) and (iii). The electrical conductivities of PCN and analogous materials are closely tied to their PEC properties. Enhancing crystallinity can improve conductivity, and recent studies have shown promising progress in crystalline carbon nitride materials.<sup>58</sup>

In short, controlling the synthesis conditions is the key to modulating the crystallinity of a given C<sub>3</sub>N<sub>4</sub>, thereby affecting the physical and chemical properties of the structure. When considering any semiconductor, including carbon nitrides, for PEC applications, the first key factor to consider is light absorption. The photons are converted to charge carriers through irradiation with sufficient energy to equate or surpass the  $E_g$  value.<sup>59</sup> The bandgap on the carbon nitrides is formed predominantly by  $\pi-\pi^*$  transitions in the conjugated aromatic system, and usually this transition starts at wavelengths of ca. 460 nm. The upper limit of the valence band (VB) aligns with the highest occupied molecular orbital (HOMO), while the lower limit of the conduction band (CB) aligns with the lowest unoccupied molecular orbital (LUMO). The transport of the charge carriers in C<sub>3</sub>N<sub>4</sub> occurs differently than most inorganic semiconductors such as ZnO and TiO<sub>2</sub>, with the generation of electron/hole ( $e^-/h^+$ ) pairs moving freely through the CB and VB of more ordered crystal structures. The literature suggests that in C<sub>3</sub>N<sub>4</sub> the charge transport occurs more similarly to other organic materials, described through the hopping mechanism of electron and hole polarons,<sup>60,61</sup> a phonon-assisted tunneling mechanism, allowing charge carriers to move between sites. Lochbrunner et al. pointed out that the mobility of these phonons exceeds  $10^{-5} \text{ cm}^2 \text{ V}^{-1} \text{ s}^{-1}$ ,<sup>60</sup> which is comparable to that of most organic semiconductors.<sup>62–66</sup> However, it is lower by several orders of magnitude than that of conventional semiconductors<sup>67–70</sup> where  $e^-/h^+$  mobility is characterized by band transport.

In photoredox reactions, not only the  $E_g$  value but also the energetic positions of VB and CB are significant. Some reports from theoretical calculations regarding the band structure of carbon nitrides indicate that both C 2p and N 2p orbitals contribute to the CB, while the VB is mainly formed by the N 2p orbitals.<sup>71,72</sup> Thus, altering the C/N ratio of a given carbon nitride affects the interaction between these orbitals, thereby modulating the energy levels of both the CB and VB.<sup>71,73</sup> Controlling the  $E_g$  and the band position through the synthesis is one of the criteria for the ability of a material to both absorb photons and further transfer the generated charges, performing specific photoredox reactions. In other words, the positions of the CB and VB determine how feasible a given photocatalytic

reaction can be. For the determination of flat-band ( $E_{\text{FB}}$ ) potential, and consequently CB and VB values, various approaches are found in the literature,<sup>74,75</sup> such as Mott–Schottky,<sup>73,76</sup> illuminated chronopotentiometry,<sup>77</sup> the Butler and Ginley relationship,<sup>78</sup> among others. Each of these methods has its limitations and pitfalls, with the values obtained capable of exhibiting significant variation within the same sample depending on the technique used. Selishchev and co-workers reported four different methods to determine the  $E_{\text{FB}}$  of the same sample of PCN synthesized from the pyrolysis of urea.<sup>75</sup> The techniques included Mott–Schottky, illuminated chronopotentiometry, photocurrent onset, and Gartner–Butler. The values obtained were  $-0.25$  V,  $0.10$  V,  $-0.60$  V, and  $-0.66$  V versus the reversible hydrogen electrode (RHE), respectively. Due to the high porosity of carbon nitrides and challenges in developing the space charge layer, Mott–Schottky experimental data deviates from a linear dependence, making it less suitable for determining  $E_{\text{FB}}$ .<sup>79</sup> Results from the illuminated chronopotentiometry method also show even greater disparities than other findings. The authors attribute these disparities to the experimental conditions of the study on PCN, in which it was incapable of reaching a high level of flat-band potential.

Furthermore, it is possible to find studies that indicate a variation of the CB potential for conventional  $\text{C}_3\text{N}_4$  from approximately  $-0.7$  V to  $-1.53$  V vs RHE, while for the VB the potential varies from  $1.03$  to  $1.90$  V vs RHE.<sup>54,73,78,80</sup> In turn, ionic carbon nitrides typically achieve more positive conduction band potentials due to the organization of melam and melam intermediates during synthesis,<sup>81,82</sup> and for instance, can enable a higher production of  $\cdot\text{O}_2^-$  radicals. In practical photoelectrocatalytic applications, these band values indicate that both conventional and ionic carbon nitrides possess a suitable band structure for performing many important reactions, such as water splitting,<sup>83</sup>  $\text{CO}_2$  and  $\text{N}_2$  reduction,<sup>84,85</sup> among others.

The controlled insertion of defects or doping of the structure can also be beneficial in carbon nitride performance. The generation of vacancies, structural defects, and doping can modulate the characteristics of a  $\text{C}_3\text{N}_4$  in a similar way as observed for inorganic semiconductors,<sup>39</sup> once it can insert deep-level defects into the structure, trapping photogenerated carriers, reducing charge recombination at some extent.<sup>86,87</sup> Figure 3 presents the band diagrams of different types of PCNs reported in the literature,<sup>39,88,89</sup> within the redox potential of some reactions of interest. It is possible to observe that doping with elements such as iodine allowed a considerable reduction in  $E_g$ , while other nonmetals—such as sulfur and phosphorus—despite presenting a smaller variation in the band gap, displace the position of their VB and CB considerably in comparison to the unmodified PCN. The electronic properties can, in general, be dramatically affected by the doping of a semiconductor. Among the most commonly employed elements to induce positively charged defects are originated from groups with fewer electrons than carbon, like boron,<sup>90</sup> and to induce negatively charged defects we can use elements such as fluorine,<sup>91</sup> sulfur,<sup>92</sup> or oxygen.<sup>93,94</sup>

Nitrogen vacancies can be generated during or after the synthesis by thermal treatments by controlling the temperature and atmosphere of the system.<sup>95–97</sup> Upon nitrogen atom release from the carbon nitride structure, the neighboring carbon atoms can stay uncoordinated for some time or lead to new  $\text{C}=\text{C}$  bonds. Regardless of charge trapping, the resulting

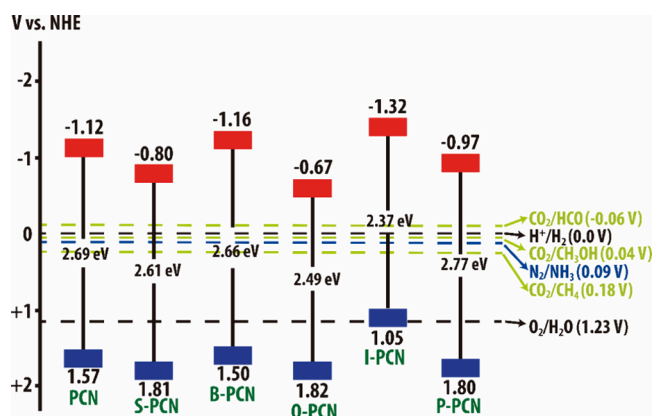


**Figure 3.** Schematic illustration of the band structures of PCN samples with different nonmetal doping and some possible redox reactions. Reproduced with permission from ref 39. Copyright 2015 John Wiley and Sons.

modification in the energy levels affects the interaction with substrates sharply and the electronic conductivity.<sup>98</sup> Increasing the number of  $\text{C}=\text{C}$  bonds within the structure can improve the electronic conductivity, which is poor for pristine  $\text{C}_3\text{N}_4$ .

Furthermore, this obstacle can be overcome by combining or mixing with conductive materials such as graphene-derived materials. Shalom and co-workers obtained hybrid films between PCN and reduced graphene oxide (rGO) from the thermal condensation of a mixture of cyanuric acid-melamine and graphene oxide.<sup>99</sup> The new PCN-rGO films exhibited improved conductivity, with the rGO acting as an electron-accepting layer (EAL) which allows for effective electron transfer to the substrate. Due to a higher diffusion length, the recombination rate was drastically reduced, resulting in a photoelectrochemical performance 20 times higher than that of pristine PCN.

Coordinating transition metal ions, such as those in the previously mentioned work of single atom,<sup>41</sup> can lead to localized surface defects that can trap photogenerated charge carriers. The insertion of ions/atoms provides additional binding functions, which endow PCNs with unique properties by lowering the  $E_g$ , enhancing the absorption of visible light, or acting as a cocatalyst (Cocat). The charge balance and the size of the ion affect the structure of the PCN.<sup>44,100</sup> This is a pathway for structural engineering of the PCN crystalline structure, as demonstrated by Lin et al. due to the presence of charged  $\text{Li}^+$  on PTI. Metals such as cobalt and platinum deposited on the surface  $\{1\ 0\ \bar{1}\ 0\}$  could modulate the electron hopping potential. In other words, the interlayer electron hopping potential is much higher than the in-plane potential, favoring any charge transfer process on the carbon nitride layer and leading to an improved photoresponse on the prism side crystal facets. Even small distortions in the crystalline structure can affect the spatial separation of the charge carriers. For example, the insertion of Mo by thermal condensation, as demonstrated by Cui et al. led to a carbon nitride with a lower recombination rate, a huge redshift on the  $E_g$  (down to  $1.4$  eV), and displacement on the material band edges enough to perform effectively reduction reactions.<sup>101</sup> The distortions on the crystal structure pointed with ion doping are indicative of how changes in the morphology can also affect the photo-response of a PCN. If the material is synthesized as a bidimensional sheet, the diffusion of the charge carriers to the

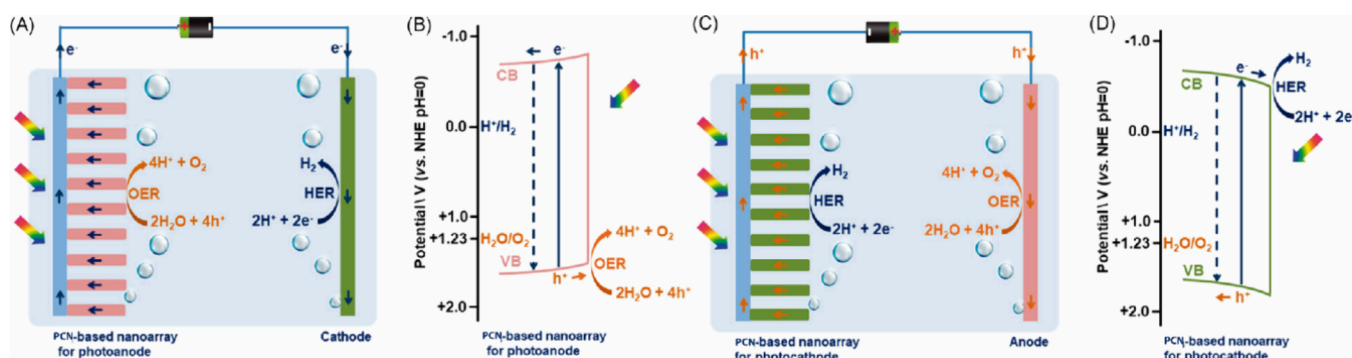


**Figure 4.** Schematic of PEC water-splitting cell using a PCN-based nanoarray as (A, B) photoanode and (C, D) photocathode, respectively. Reproduced with permission from ref 56. Copyright 2020 John Wiley and Sons.

surface is facilitated,<sup>102</sup> as can be observed by the changes in the photoluminescence lifetimes.<sup>103</sup>

The combination with a proper cocatalyst can enhance the  $C_3N_4$  properties. For instance, coupling with plasmonic nanoparticles can serve as a physical amplifier for the response due to high light scattering, or due to a Schottky barrier formation.<sup>104,105</sup> This is particularly valuable in sensing applications, as it improves the photocurrent response, as observed in a heterojunction of CdS/PCN coupled with noble Au@Ag nanoparticles and DNAase for microRNA bioanalysis, due to the phenomenon of exciton–plasmon interactions (EPI).<sup>106</sup> In this case, the sensor demonstrates subfM level detection, approximately 0.05 fM of microRNA-21, within a range of 1.0 nM to 0.1 fM.

Inserting elements and/or functional groups as dopants modulates the physicochemical properties of PCNs, and these species can act as cocatalysts assisting the desired photoelectrochemical processes. Factors such as ion charge, acidity, or alkalinity can influence the interaction of the PCN with the substrate, becoming active sites for the reaction, and mainly favoring the charge transfer process, decomposing reaction intermediates, and even reducing the overpotential required for a reaction.<sup>107–109</sup>

Using molecular dopants is also an alternative to heteroatoms, *i.e.*, functionalizing the  $C_3N_4$  structure with groups rich in  $\pi$ -conjugated electrons such as thiophene, diamines, and acids. Due effects of injecting/withdrawing electrons and changing the electronic orbital interactions through  $C_3N_4$  directly affect the  $E_g$  value and the band position. The functionalization with thiophene reduces the  $E_g$  value of PCN to 1.7 eV.<sup>110</sup> In the work of Bian et al.<sup>111</sup> it is shown that copolymerizing melamine with a pyridine derivative produces modified carbon nitride films that achieve a photocurrent up to  $100 \mu A cm^{-2}$  (at 1.23 V vs RHE).

In addition to the structural approaches commented on previously, controlling the morphology of the electrode also has a great influence on the PEC properties. Fabricating one-dimensional structures and highly ordered arrays<sup>56,112</sup> may lead to enhanced charge transport associated with a higher surface area where more active sites are available. One good example found in the literature is PCN-based nanoarray photoelectrodes.<sup>55</sup> Beyond the cited advantages, the PC possesses a band position suitable for both reduction and oxidation, *i.e.*, as a photoanode and photocathode, as shown in Figure 4. When compared with mesoscopic photoelectrodes made by PCN nanoparticles, highly ordered nanoarrays can afford much faster transport pathways for carriers, avoiding

localized recombination at the grain boundaries.<sup>113</sup> Furthermore, ordered structures like the ones described above are ideal platforms to build heterostructures, to enhance the material performance even more.

One critical challenge faced by semiconductors, including carbon nitrides, when used in photoelectrochemical cells, is the quality of the film. The deposition of uniform and homogeneous films with good adherence to the substrates of interest is fundamental for the accurate photoelectrochemical evaluation of a given  $C_3N_4$ . Deposition methods can be divided into two main methods as illustrated in Figure 5: (i) powder

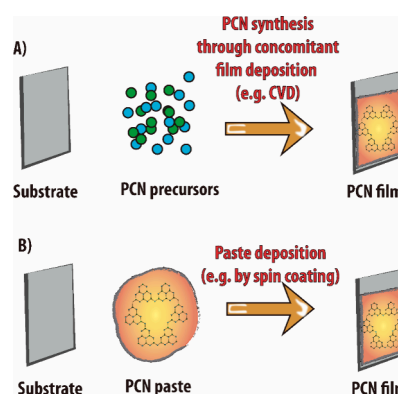


**Figure 5.** Schematic representation of (A) *in situ* and (B) *ex situ* methods of PCN film preparation.

preparation followed by deposition (*ex situ*)<sup>114</sup>—such as spin coating, dip coating, and electrophoretic deposition; or (ii) direct growth on a given substrate of interest (*in situ*),<sup>115,116</sup> like gas phase deposition techniques.<sup>57</sup> There is no consensus on an ideal method (*ex situ* or *in situ*), while methods such as chemical vapor deposition (CVD) allow obtaining thin layers of dense PCN, the material crystallinity will depend on the epitaxial growth in a given substrate.<sup>57</sup> *Ex situ* methods usually have less contact with the support, being more susceptible to leaching, but allow greater control of the material synthesis prior deposition allowing improved and detailed control of the intrinsic properties of the PCN. Increasing a  $C_3N_4$  film thickness can also increase light absorption, but at the same time, the greater the film thickness, the longer the path the charges need to travel, increasing the chance of recombination.

After engineering the micro- and macrostructural modifications to enhance PCN photoresponse (doping, vacancies, *etc.*), combining it properly with other semiconductors can lead to

the ultimate improvement of the photoelectrochemical properties. Heterojunctions can enhance charge separation and, thus, photoelectrochemical reactions. However, the band position between the chosen semiconductors must be considered carefully. There are plenty of semiconductors with band positions that favor building a type II heterojunction with polymeric carbon nitrides, *i.e.*, with both the CB and VB above or below the respective bands of the carbon nitride. An example is the combination with  $\text{Fe}_3\text{O}_4$ <sup>117</sup> or  $\text{BiVO}_4$ .<sup>118</sup> As per May,<sup>119</sup> owing to the differences in the electrochemical potential of both materials, the band edge may be upward or downward bending. Consequently, a gradient of electrochemical potential is established, serving as a driving force that enhances the spatial separation of charge carriers. Throughout excitation, recombination, and charge extraction,  $e^-$  and  $h^+$  are added to or removed in equal numbers. Therefore, any change in free energy resulting from carrier extraction is the sum of the electrochemical potentials of the exchanged charge carriers and can be further identified as the difference in the quasi-Fermi levels. Depending on the band alignment and the difference in the quasi-Fermi levels, the photocurrent performance can increase up to 10 times higher than for bare  $\text{C}_3\text{N}_4$ .<sup>118</sup>

In electrode engineering, it is possible to use a combination of two or more approaches, where Figure 6 presents some

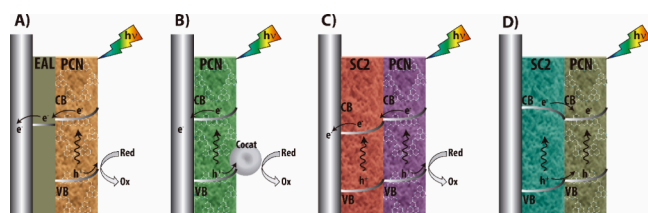


**Figure 6.** Representation of some PCN photoanode interfaces: (A) containing an electron accepting layer, (B) cocatalyst (Cocat), (C) type II, and (D) type I heterojunction. The band bending was arbitrarily drawn for illustration purposes only.

possible architectures for PCN-based photoelectrodes. Figure 6A presents the use of an EAL where, due to the favorable conduction band energy of the EAL, the migration of photogenerated electrons occurs, increasing charge separation. Figure 6B presents the use of a cocatalyst as an intermediary for the redox reaction. Figure 6C and D present illustrated type II and I heterojunctions of a PCN with a second semiconductor (SC2). The second case is unwanted due to its effect of driving charge carriers in the same direction, increasing the level of recombination. The kind of energy band alignment represented in type II can be also achieved between PCNs with different band gaps, which can be called a homojunction. As an example, we mention the doping of one PCN with boron and its combination with an undoped nitride. The obtained material presented significantly increased photoresponse, in which not only the charge separation but also the transfer along the electrode/electrolyte interface improved.<sup>120</sup>

### 3. PHOTOELECTROCHEMICAL APPLICATIONS

**3.1. Water Splitting.** A common application of semiconductors in PEC is water-splitting, whereupon the reduction (hydrogen evolution) and the oxidation (oxygen evolution) reactions are performed simultaneously but are spatially

separated at the (photo)anode and (photo)cathode. By using a cell with a PCN as a photoanode, the  $e^-/h^+$  pair is generated after photoexcitation; then, the charges are separated and driven in opposite directions by the applied bias. The holes oxidize water at the photoanode surface, conducting an oxygen evolution reaction (OER), while the electrons must travel through the external circuit to the counter electrode to drive the hydrogen evolution reaction (HER).

Considered a clean and sustainable dense energy carrier,  $\text{H}_2$  is the main goal of PEC water splitting to substitute for fossil fuels.<sup>121</sup> As the CB and the VB of PCNs can, in most cases, surpass the redox potential of  $\text{H}^+/\text{H}_2$  and  $\text{H}_2\text{O}/\text{O}_2$ , polymeric carbon nitrides represent suitable materials for overall water splitting. To assess the efficiency of the photoelectrode, various methods can be found in the literature. These methods include  $\eta_{\text{transfer}}$ , which involves comparing the photocurrent in the presence and absence of hole or electron scavengers; IPCE, where the photocurrent is evaluated as a response to a monochromatic light source; applied bias photon-to-current efficiency (ABPE), which considers the applied potential instead of the light source; and solar-to-hydrogen (STH), considered the primary parameter for water splitting as it represents the ratio of the produced hydrogen to the incident solar energy, under zero bias.

To our knowledge, the first report involving a PCN-based photoanode was made in 2010 by Zhang and Antonietti.<sup>122</sup> The study presented different systems of PCN nanostructured films, including mesoporous carbon nitride, Fe-doped PCN, and bulk PCN, either alone or in binary combinations with an electron-transport medium ( $\text{TiO}_2$ ) or a hole-transport medium (poly(3,4-ethylene dioxythiophene - PEDOT). Photocurrents serve as a significant parameter for evaluating material efficiency, and in this case, the authors reported values of approximately  $50 \mu\text{A cm}^{-2}$  as the best result obtained for carbon nitrides alone. In the binary films, light-generated excitons were more effectively dissociated through the hole or electron transport medium, achieving photocurrents of  $90 \mu\text{A cm}^{-2}$  for electrodes containing PEDOT-PSS and  $150 \mu\text{A cm}^{-2}$  for those containing  $\text{TiO}_2$ . The IPCE reached 3% in the last case, a value considered high even when compared to some bare inorganic semiconductors.<sup>123,124</sup>

Currently, the efficiency of PCN-based PEC devices is still low due to reasons such as fast recombination of photoexcited charges, poor electronic conductivity, and limited charge carrier diffusion. To overcome these limitations and enhance performance, some photoanode architectures have been proposed. In the work of Karjule, PCN was the photoactive layer, while rGO was used as an EAL, in addition to a metal-organic framework (MOF) containing nickel and iron as a cocatalyst for oxygen evolution reaction (OER).<sup>125</sup> As the PCN had a CB potential more negative than that of the EAL, it allowed efficient electron injection from the polymeric carbon nitride, leading to a larger number of holes available for water oxidation. The use of nanostructured electron-transporting paths, such as nanowires and nanotubes, incorporated within the active layer can separate light absorption from charge-carrier migration. By doing so, recombination can be further hindered by the EAL, since the necessary electron diffusion lengths are shorter than the thickness of the absorbing PCN layer.

Titanium dioxide is among the most exploited heterojunctions with  $\text{C}_3\text{N}_4$  for both photoanodes<sup>126,127</sup> and photocathodes,<sup>128</sup> due to the high results achieved. In some cases,

where carbon nitride was deposited on the surface of TiO<sub>2</sub> nanorods, a significant 21-fold increase in photocurrent was observed compared to the bare materials.<sup>129</sup> The improved performance was attributed to longer electron lifetimes in the active material, and similar results were obtained for TiO<sub>2</sub> nanotubes modified with carbon nitrides or P-doped PCN. In both cases, photocurrent densities in the order of mA cm<sup>-2</sup> were reached.<sup>130,131</sup> Coupling carbon nitride with TiO<sub>2</sub> offers an additional benefit of the metal oxide serving as an electron collector. This simultaneous interaction allows both materials to photogenerate charges spatially separated between two phases with distinct electronic properties while maintaining stability.

Transient absorption spectroscopy (TAS) measurements can help determine the lifetime of charge carriers as well as show the charge injection rate from PCN into other semiconductors. From the carbon nitride to TiO<sub>2</sub>, for example, the charge injection is on the nanosecond order, being more than a hundred times faster than in the backward direction,<sup>132</sup> in this case, however, the hole extraction rate is limiting the overall performance of the PEC. As the combination with TiO<sub>2</sub> shows good potential, Beranek et al. aimed to further enhance the PEC behavior of a TiO<sub>2</sub>-PHI heterojunction by investigating the incorporation of Co(II/III) cocatalytic sites.<sup>133</sup> Density-functional theory (DFT) calculations predict the adsorption of Co(II/III) ions in nanocavities at the heterojunction surface. The binding of Co ions leads to TiO<sub>2</sub>-PHI/Co(II) photoelectrodes exhibiting efficient coupling to photogenerated holes, resulting in complete water oxidation.

The absorption range and charge separation efficiency of PCN materials could be increased by Z-scheme, a special type of heterojunction mimicking natural photosynthesis. This is demonstrated in the Z-scheme fabrication between PCN, p-ZnO, and MnO<sub>2</sub> (p-ZnO/PCN/MnO<sub>2</sub>) obtained in three steps: (i) thermal polymerization; (ii) electrodeposition; and (iii) partial etching,<sup>134</sup> presented in Figure 7. In this photoanode, the polymeric carbon nitride and manganese dioxide were encapsulated on zinc oxide nanorods, and while the ZnO acts as a charge collector, the MnO<sub>2</sub> protects the PCN from oxidation, improving the stability of the sample. The photocurrent density obtained from the OER was 5.2 mA

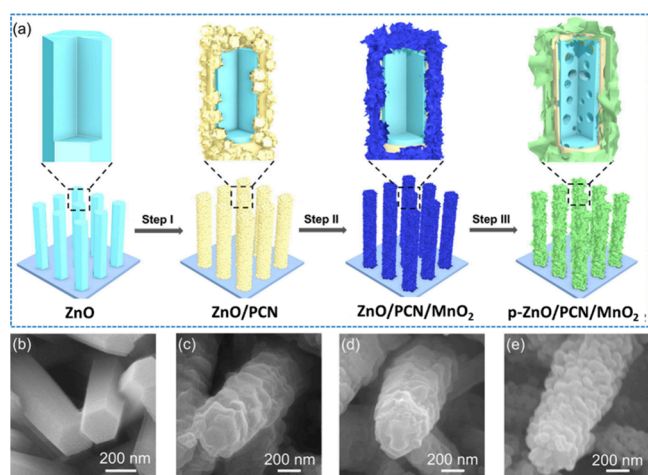
cm<sup>-2</sup>, at low onset potential (0.6 V vs Ag/AgCl), which indicates a high efficiency of the system.

Table 1 presents a compilation of some of the best results found in the literature for photoelectrodes (photoanodes and photocathodes) based on PCN that has been utilized in water splitting,<sup>55,57</sup> demonstrating how PCN materials can be effectively utilized in diverse situations, particularly with the right material modifications. A relevant difference between the values reported for photocurrent is observed, ranging from micro to milliamps, and is possible to correlate the photocurrent values and the efficiency with PCN modifications, from bare PCN electrodes some are increasing, especially if the semiconductor has a notoriously high efficiency as is the case with silicon.<sup>135</sup> The benchmark value of the photocurrent (5 mA cm<sup>-2</sup>) was reported for the architecture ZnO/PCN/Co-Pi and the combination of heterojunction and the use of a cocatalyst showed that for the good performance required a smart arrange of strategies.<sup>136</sup> Another parameter exhibiting significant variation is stability time tests, which in some cases are reported with less than 10 min, however, in the heterojunction with CuInS<sub>2</sub> the reported chronoamperometry test lasted for 22 h.<sup>137</sup> Efficiency reports are less comparable because they were evaluated under different parameters. Nevertheless, systems such as the Ti-Fe<sub>2</sub>O<sub>3</sub>/PCN achieving 9% IPCE efficiency, can be considered one of the most promising due to the utilization of visible radiation (400 nm).<sup>138</sup>

It is worth highlighting the versatility of PCN, as it can also be applied in photoanodes and cathodes, such as in combination with NiO or with CuInS<sub>2</sub>.<sup>137,139</sup> In low overpotentials (0.42 V vs RHE), the NiO/PCN heterojunction successfully suppressed charge recombination, resulting in a photocurrent of -70 μA cm<sup>-2</sup>. In combination with the p-type CuInS<sub>2</sub>, the carbon nitride inhibited the photocorrosion of the chalcopyrite, at the same time it reduced the photocurrent onset in ca. 0.15 V.

**3.2. Biomass Upgrading.** One challenge in the overall water splitting is the sluggish oxygen evolution reaction, which adds to the required potential for the overall reaction (1.23 V). This results in the scientific community looking for alternative oxidation reactions. Despite usually having lower oxidation potentials in comparison to OER, oxidizing selectively biomass sources can produce high-value chemicals, e.g., fuels, intermediates for industry, and fine chemicals,<sup>18,148</sup> while at the same time supplying the electrons for the hydrogen evolution. Regardless of the advantages and potential, photoelectrochemical biomass upgrading is still at an early stage, facing some challenges. First, the chemical composition of biomass, which is diverse and can vary dramatically depending on the source, stimulates work with more purified and well-defined derivatives. For example, vegetal biomass sources such as agricultural residues and food waste can be composed of polysaccharides, lignin, lipids, proteins, and inorganic compounds, but with different compositions.<sup>149-151</sup>

The second main challenge is the selectivity during the photoredox process, avoiding overoxidizing the products and the formation of any passivation product that could cover the surface of the photoelectrode making it unusable. Selective and efficient oxidation of a given organic group is appealing but at the same time quite difficult. Glycerol is a good example of a biomass-derived product obtained as a byproduct from the biodiesel industry, as it has the potential to be a platform for the synthesis of many chemicals. This molecule is a polyol with



**Figure 7.** (A) Representation of the p-ZnO/PCN/MnO<sub>2</sub> growth, SEM images of (B) ZnO, (C) ZnO/PCN, (D) ZnO/PCN/MnO<sub>2</sub>, and (E) p-ZnO/PCN/MnO<sub>2</sub>. Reproduced with permission from ref 134. Copyright 2019 Elsevier.

Table 1. Water Splitting Parameters Reported for PCN-Based Photoelectrodes in the Literature

Photoelectrode	Electrolyte	Scavenger	Light source	Photocurrent (mA cm <sup>-2</sup> )	Max efficiency (%)	Stability time (min)	Source
S-doped PCN/Bi <sub>2</sub> WO <sub>6</sub>	KOH (1.0 M)	No	AM 1.5G, 100 mW cm <sup>-2</sup>	0.057 at 1.23 V vs RHE	0.017 at 1.23 V vs RHE (ABPE)	10	108
Si/PCN	H <sub>2</sub> SO <sub>4</sub> (0.05 M)	No	AM 1.5G, 100 mW cm <sup>-2</sup>	0.65 at 1.5 V vs SCE	-	-	135
ZnO/PCN/Co-Pi	NaCl (3.5 wt %)	No	White light 400 mW cm <sup>-2</sup>	5.0 at 1.23 V vs RHE	-	10	136
CuIn <sub>2</sub> /pcn	H <sub>2</sub> SO <sub>4</sub> (0.1 M)	No	AM 1.5G, 100 mW cm <sup>-2</sup>	-0.15 at -0.35 V vs RHE	-	1320	137
Ti-Fe <sub>2</sub> O <sub>3</sub> /PCN	NaOH (1.0 M)	No	Visible light	2.55 at 1.23 V vs RHE	9 at 400 nm (IPCE)	5	138
NiO/PCN	Na <sub>2</sub> SO <sub>4</sub> (0.2 M)	No	Visible light	-0.07 at 0.42 V vs RHE	-	5	139
TiO <sub>2</sub> /PCN	KOH (1.0 M)	No	AM 1.5G, 100 mW cm <sup>-2</sup>	0.142 at 1.23 V vs RHE	0.072 (STH)	10	140
PCN	KCl (1.0 M)	No	AM 1.5G, 100 mW cm <sup>-2</sup>	0.02 at 0.8 V vs Ag/AgCl	-	-	141
TiO <sub>2</sub> @PCN	Na <sub>2</sub> SO <sub>4</sub> (0.1 M)	0.01 M H <sub>2</sub> O <sub>2</sub>	UV-visible	0.08 at 0.8 V	90 ( $\eta_{\text{transfer}}$ )	5	142
WO <sub>3</sub> /pcn	Na <sub>2</sub> SO <sub>4</sub> (0.2 M)	No	AM 1.5G, 100 mW cm <sup>-2</sup>	2.1 at 2 V vs RHE	53.1 at 350 nm (IPCE)	-	143
CdS@PCN	Na <sub>2</sub> SO <sub>3</sub> (0.35 M) and Na <sub>2</sub> S (0.25M)	SO <sub>3</sub> <sup>2-</sup> and S <sup>2-</sup>	AM 1.5G, 100 mW cm <sup>-2</sup>	1.16 at 0.9 V vs RHE	-	60	144
PCN-rgo/NiFeO <sub>x</sub> H <sub>y</sub>	KOH (0.1M)	TEOA (10%)	AM 1.5G, 100 mW cm <sup>-2</sup>	0.5 at 1.23 V vs RHE	32 at 380 nm (IPCE)	4	145
N-doped carbon dots@Fe <sub>2</sub> O <sub>3</sub> /PCN	Na <sub>2</sub> SO <sub>4</sub> (0.1 M)	No	Xe lamp with UV filter, 100 mW cm <sup>-2</sup>	3.07 at 1.6 V vs RHE	0.32 (STH)	6	146
CuO/PCN	Na <sub>2</sub> SO <sub>4</sub> (0.5 M)	No	AM 1.5G, 100 mW cm <sup>-2</sup>	0.6 at 1.2 V vs Ag/AgCl	-	1	147

different hydroxyl groups (CH<sub>2</sub>OH-CHOH-CH<sub>2</sub>OH), in the edge of the structure (terminal hydroxyls) and the middle, but, as each group, has different reactivity, consequently challenging the selective conversion to a value-added product like dihydroxyacetone (CH<sub>2</sub>OH-CO-CH<sub>2</sub>OH). By supporting gold nanoparticles in a carbon nitride photoanode, Sun et al. attempted to obtain dihydroxyacetone with a selectivity higher than 50%. It was possible due to a cooperative dual injection effect between localized surface plasmon resonance effect in Au injecting electrons to the CB of the PCN, and further to the external circuit, with a continuous injection of the photo-generated holes from the PCN to the Au nanoparticles, which consequently lead to a turnover frequency of 4.62 h<sup>-1</sup>.<sup>152</sup>

Some findings from our group include a photoanode between TiO<sub>2</sub> and PHI containing Ni<sup>2+</sup> single sites (TiO<sub>2</sub>-Ni-PHI) that were employed for methanol (MeOH) PEC oxidation.<sup>153</sup> The photoanode was quite stable and showed a cooperative effect between TiO<sub>2</sub> and Ni-PHI, where the type-II heterojunction between TiO<sub>2</sub> and PHI improved charge separation, while the nickel sites performed cocatalysis for methanol oxidation, improving charge transfer. Under optimized conditions, e.g., UV light, 58% V: V of MeOH TiO<sub>2</sub>-Ni-PHI reached almost 11 mA cm<sup>-2</sup> at 0.6 V vs RHE. By combining PEC with an *in situ* FTIR measurement, we observed that without light TiO<sub>2</sub>-Ni-PHI only oxidized MeOH to formaldehyde (an oxidation process involving two-electrons), and under light, MeOH was converted after 0.3 V vs RHE to formic acid (four electrons), a valuable compound for the fine chemical industry. On higher potentials, MeOH was then converted to CO<sub>2</sub> (6 electrons), showing that the product can be selectively controlled.

Glucose, an important biomass resource was oxidized to gluconate through PEC by an unusual architecture: a Pt electrode, covered with PCN containing Pt nanoparticles, then

coated with a polymer of intrinsic microporosity (PIM-1).<sup>154</sup> The PIM-1 coating assured better mechanical stability of the PCN@Pt film despite the generation of an important pharmaceutical industry intermediate (gluconate). The overall reaction was based on H<sub>2</sub> production, which was oxidized at the Pt electrode enhancing the current response of the system.

As pointed out in Section 2, one issue for good PEC responses on PCN films is having good adhesion between the polymeric carbon nitride and the conductive substrate. Figure 8 summarizes a study with a new approach to overcoming the adhesion problem. By a sol-gel method using a water-soluble PHI precursor, a noncovalent hydrogel was formed and deposited over the FTO electrode.<sup>81</sup> The PHI film obtained

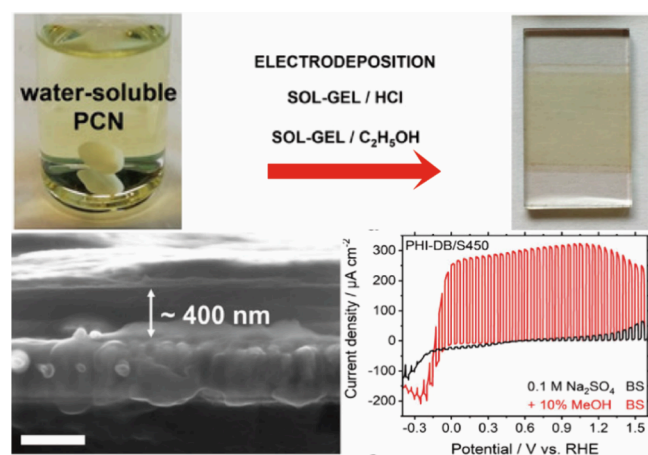


Figure 8. Representation of the synthesis of PHI films with good adhesion, controlled thickness, and high photocurrent from methanol oxidation. Reproduced with permission from ref 81. Copyright 2021 John Wiley and Sons.



was used for PEC alcohol reforming, and it is noteworthy that a very low photocurrent onset was achieved. This is significant when considering the reduction of operational costs, since it enables the electrode to operate under zero bias. Furthermore, this electrode demonstrated the effect of photodoping, as observed elsewhere.<sup>49</sup>

Upgrading biomass by the photoelectrochemical process represents some feasible advantages for biomass valorization and other desired chemical conversions. It can be considered a green route due to its operation, in general, under mild (voltage, temperature, and pressure) conditions. And by the possibility of generation of any oxidative or reducing equivalent without the addition of any external and toxic reagents, enabling access to difficult chemical transformations without imposing harsh protocols.

**3.3. Environmental Remediation and Sensing.** Many reports suggest PCN in photocatalysis and photoelectrocatalysis as a green route for environmental remediation due to the potential for both direct (by oxidation) and indirect (by the generation of reactive oxygen species) degradation of organic pollutants. However, there is less exploration of the potential of semiconductors. In general: using the electrons from pollutant oxidation to generate H<sub>2</sub> and recover part of the energy used for the degradation. This is not a simple task because the PCN photoanodes can suffer poisoning by any recalcitrant products of degradation and the photoelectrochemical cell must have separated compartments for the oxidation and the reduction reactions to attain H<sub>2</sub> with higher purity.

Organic dyes are an important class of pollutant models that can be employed in the evaluation of the PEC activity for contaminant degradation. The aforementioned p-ZnO/PCN/MnO<sub>2</sub> Z-scheme with high values of photocurrent for water splitting (*ca.* 5 mA cm<sup>-2</sup>) also performed methylene blue degradation, achieving a rate constant of 0.035 min<sup>-1</sup> and a degradation percentage higher than 88%. This demonstrates how a smart electrode architecture can be versatile and perform in multiple applications.<sup>134</sup>

The antibiotic ciprofloxacin (CIP) is among the emerging pollutants and can be found in wastewater resources in concentrations up to 125 μg L<sup>-1</sup>.<sup>155</sup> Qin et al.<sup>156</sup> pursued the CIP degradation by a photoanode composed of a PCN and a metal–organic framework containing iron (PCN/MOF(Fe)) synthesized by a solvothermal route. Terephthalic acid was used as a linker between the two compounds, and the obtained electrode performed CIP degradation even on real wastewater samples through a cooperative effect between enhanced photoelectrocatalysis, due to favorable band alignment on the heterojunction, and electro-Fenton process on the Fe<sup>II</sup>/Fe<sup>III</sup> sites generating the oxidizing species •OH and h<sup>+</sup>.

Furthermore, reinforcing the importance of vacancy generation on PCN is the fact that it can play an important role in altering its catalytic properties, as observed in 4-chlorophenol (4-CP) degradation by a PCN electrode with nitrogen vacancies. By using mild conditions such as simulated sunlight and 0.8 V enhanced 4-CP, degradation was achieved by the referred photoanode. It is mainly due to the effect of N-vacancies narrowing the material band gap while acting as trapping for photogenerated charge carriers and favoring the 4-CP adsorption, which resulted in a mineralization of almost 80% after 2 h.<sup>96</sup>

The increasing environmental pollution has produced threats to public health, and it is critical to develop cheap and efficient technologies such as PCN-based processes for

remediation as well as to develop sensors for efficient monitoring. Despite degradation use, the photocurrent response sometimes is not high enough for uses such as energy conversion. However, in some cases, it is linear with the target molecule concentration, allowing us to sense quantitatively this kind of compound. 4-CP was monitored and degraded by a P-doped carbon nitride electrode containing gold nanoparticles (Au/P-PCN). The photoelectrode synthesis and application are represented in Figure 9, due to the

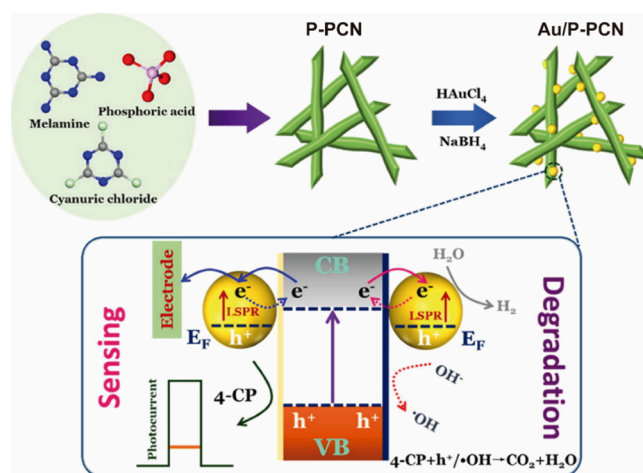


**Figure 9.** Schematic of synthesis and application of Au/P-PCN for sensing and degrading 4-CP. Reproduced with permission from ref 157. Copyright 2023 Elsevier.

localized surface plasmon resonance (LSPR) effect from Au nanoparticles acting as an amplifier of the absorbed light; it further enhanced the signal of the sensor, which resulted in a sensor with a linear range of 0.1–52.1 μM. At the same time, with the photoexcitation where were produced •OH, and h<sup>+</sup> oxidizing species, which led to a removal efficiency of ~87% of 4-CP, combining on the same material the capability to measure and degrade a compound through PEC.<sup>157</sup>

As C<sub>3</sub>N<sub>4</sub> materials are composed of stacked layers, exfoliation routes can be used to make graphene analogs, *i.e.*, 2D layers with few sheets stacked and a high surface area. Xu et al. prepared a PCN intercalated with NH<sub>4</sub>Cl,<sup>158</sup> further by a thermal exfoliation route that obtained a thin film with 6 to 9 sheets stacked, and a large specific surface area (~30 m<sup>2</sup> g<sup>-1</sup>). The obtained carbon nitride possessed an increased band gap (2.85 eV) due to quantum confinement effects but presented good photocatalytic activity toward a model compound remotion. Most importantly, it was found that as the concentration of Cu<sup>2+</sup> increased, the photocurrent response gradually, which was in the opposite direction of other materials such as CdS and CdTe.<sup>159,160</sup> This suggests that the mechanism consists of Cu<sup>2+</sup> being adsorbed on the PCN, later acting as an electron acceptor, increasing the charge separation and so on the photocurrent. In this sense, a PEC sensor was developed to monitor copper in trace concentration, which is important once this metal is essential to living organisms but can be toxic above a certain concentration.

It was evident from the observations made that PCN materials hold great potential in terms of resourcefulness as they can be effectively utilized for generating energy from waste degradation. Moreover, their versatile nature allows for coupling environmental remediation with sensing, thus

providing an innovative solution to tackle environmental challenges.

**3.4. CO<sub>2</sub> Capture and Conversion.** One developing areas is the fixation of CO<sub>2</sub> by PEC and its conversion to value-added products. Polymeric carbon nitrides possess functional groups with catalytic functions such as Lewis basic sites. As illustrated in Figure 10, this class of versatile materials has

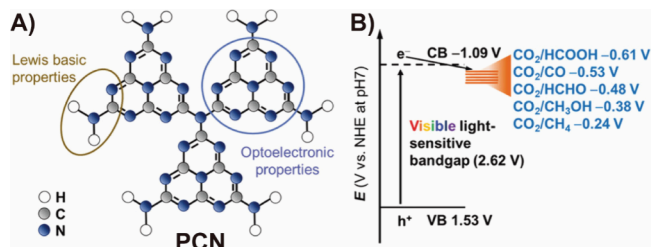


**Figure 10.** (A) Schematic of PCN useful properties for the CO<sub>2</sub>RR and (B) band diagram presenting thermodynamically feasible reactions with CO<sub>2</sub>. Reproduced with permission from ref 163. Copyright 2019 John Wiley and Sons.

emerged as attractive candidates for the CO<sub>2</sub> reduction reaction (CO<sub>2</sub>RR) and conversion into solar fuels. PEC CO<sub>2</sub>RR using PCN materials is at an early stage of research, as it is more exploratory and based on pure photocatalytic<sup>161</sup> or electrocatalytic<sup>162</sup> applications.

As represented in Figure 10, the CB position of pristine PCNs, usually approximately  $-1.1$  eV versus NHE at pH 7,<sup>163</sup> is suitable thermodynamically for CO<sub>2</sub>RR, once it is more negative than the redox potential of CO<sub>2</sub> conversion into simple C1 hydrocarbons, such as formaldehyde, formic acid, methanol, and methane. By using nanoparticles of noble metals (Pd, Pt, or Au) as cocatalysts, the architecture with PCN worked as a photocathode for CO<sub>2</sub> fixation.<sup>85</sup> The usage of a noble metal makes possible the use of a Schottky barrier due to the differences in the work function of both species (carbon nitride and noble metal), which improves charge separation and transfer. It is important to point out that in this study two photoelectrodes were tested, employing BiVO<sub>4</sub> as the photoanode (Figure 11), cooperatively with photoexcitation of the photocathode, it favored preferentially methanol formation, in a rate of  $25.1 \times 10^{-3}$  m h<sup>-1</sup> g<sup>-1</sup> and low bias application ( $-0.85$  V vs Ag/AgCl).

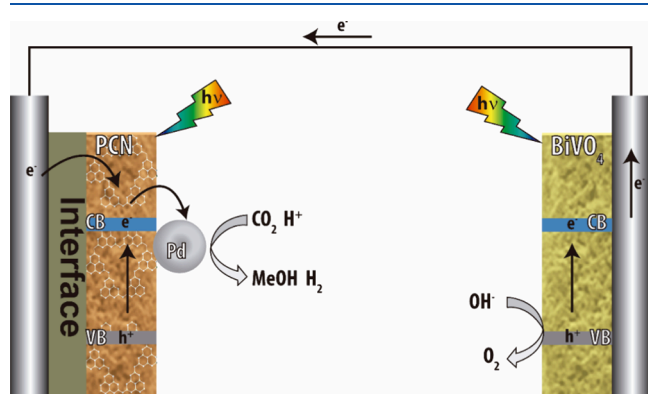


**Figure 11.** Schematic of the PEC cell employing a PCN-based photocathode and a BiVO<sub>4</sub> photoanode for CO<sub>2</sub> reduction. Reproduced with permission from ref 85. Copyright 2013 Royal Society of Chemistry.

Some prerequisites for CO<sub>2</sub> capture and further reduction are the adsorbent material showing a highly porous and stable structure as well as a high specific surface area. The pyridinic nitrogen such as on PCN structures can also be an extra benefit, enhancing the interactions with the CO<sub>2</sub> molecules. The presence of pyridinic nitrogen in the framework and NH<sub>2</sub> groups on the edges offer basic characteristics and determine its likelihood as a favorable material for CO<sub>2</sub> adsorption. It is expected that PCNs, which possess different nitrogen contents and defect sites, would exhibit better performance in terms of CO<sub>2</sub> adsorption thanks to the presence of Lewis basic sites. Coupling these properties with a highly porous structure could deliver a template for CO<sub>2</sub>RR.<sup>164</sup>

Fitting these requirements, theoretical calculations also have confirmed the potential activity of PCN materials for CO<sub>2</sub>RR.<sup>165</sup> Thus, PCN alone is thermodynamically capable of reducing CO<sub>2</sub> molecules after being photoexcited using water as a proton donor and oxidative agent. However, to be favored kinetically, the CO<sub>2</sub> reduction process relies on parameters such as reaction conditions, type of oxidative agent, input energy, and type of electrolyte employed, barriers that an adequate catalyst design can overcome. The reduction of CO<sub>2</sub> into C<sub>2</sub> and higher species is a highly desirable goal, which requires an increase in the performance of catalysts. Achieving this goal poses many challenges, due to the low catalytic efficiency of current catalysts. To overcome this limitation, a combination of theoretical first-principles, DFT calculations, and experimental studies can be used to design highly efficient catalysts, providing parameters such as the free energy and even insights into the mechanism.

A smart design of a photoelectrode was achieved by the combination of a PCN and a Zinc phthalocyanine (ZnPc) with matching energy alignment.<sup>166</sup> In this specific study, the CO<sub>2</sub>RR was performed under a combination of photocatalytic and electrocatalytic processes. There was a contribution of electrons coming from the external circuit; at the same time, the photogenerated electrons were being transferred to the adsorbed CO<sub>2</sub>, generating methanol as the major product.

Furthermore, there is still significant scope for research in exploring the potential catalytic properties of PCN in PEC applications for activating CO<sub>2</sub>, leading to the development of environmentally friendly routes for cycloaddition reactions,<sup>167</sup> among others. Although PCN-based materials have been effectively used for photoelectrocatalytic reduction of CO<sub>2</sub>, they still suffer from many problems, which could slow the reaction kinetics. However, it is a promising area of application for carbon nitrides in the green chemistry field, with capture and conversion into clean, green low-carbon fuels and valuable chemical feedstock by using sustainable and intermittent renewable energy sources of sunlight and electricity.

**3.5. Nitrogen Fixation.** The N<sub>2</sub> reduction reaction (N<sub>2</sub>RR) has an important impact from an economic and, mainly, an environmental point of view. This is due to the Haber–Bosch process, the worldwide method for NH<sub>3</sub> production method releasing 2.6 tons of greenhouse gas per 1 ton of generated NH<sub>3</sub>.<sup>168</sup> As the need for ammonia production increases (for fertilizer) on the same order as the global population, abundant and low-cost ways to convert N<sub>2</sub> to NH<sub>3</sub> production play a pivotal role in providing an affordable and stable food supply for the global population. In general, the N<sub>2</sub>RR is still in the early stages, facing some technical challenges. One such challenge is accurately evaluating the products.<sup>169,170</sup> The amount of ammonia

produced is typically small, which makes it difficult to confidently attribute it solely to correct nitrogen fixation rather than some form of contamination. Chorkendorff and co-workers have proposed a rigorous protocol for the electrochemical synthesis of ammonia, based on isotope quantification.<sup>171</sup> This protocol can be adapted for the photoelectrochemical process and is the most reliable method to unambiguously demonstrate  $N_2$  fixation.

There are two main issues with performing the  $N_2$ RR. One is that the  $N_2$  molecule possesses a thermodynamic dissociation energy of 941 kJ mol, which reduces its reactivity and process efficiency as well. The second is that the potential is similar to the required for the HER,<sup>172</sup> which leads to a competition between both reactions and asks for a catalyst material with better selectivity. In this sense, the search for an ideal materials catalyst for  $NH_3$  photoelectrosynthesis must take into consideration the nitrogen interaction on the surface of the catalyst: (i) If the interaction is too strong, the active site will be poisoned irreversibly; (ii) If the interaction is too weak otherwise, the triple bond on  $N_2$  will remain unaltered, not activating the nitrogen for further reduction. Luckily, nitrogen-rich compounds, such as nitrogen-doped carbon<sup>173,174</sup> and PCN,<sup>175</sup> due to their highly polarizable layered structure, may improve the  $N_2$ RR. When introducing electron deficient defects in the structure of  $C_3N_4$  (B-doping or C vacancies) in neighboring to the pyridinic N atoms (Lewis basic sites), they can form a frustrated Lewis pair (FLP) that results in the powerful adsorption, and subsequently, the activation of  $N_2$  molecules for ammonia formation.<sup>174–176</sup> The nitrogen reduction is favored with the presence of an FLP due to a “pull–pull effect”, reinforced by DFT calculations where the FLP forms a six-membered ring intermediate, harshly reducing the energy barrier to the cleavage of  $N_2$  molecule.<sup>177</sup>

To the present date, only two studies reported the use of  $C_3N_4$ -based catalysts on PEC  $N_2$ RR. The first was a heterojunction of PCN functionalized on  $MoSe_2$  hierarchical microflowers, that produced around  $7.7 \mu\text{mol h}^{-1} \text{L}^{-1} \text{cm}^{-2}$  of ammonia with a faradaic efficiency of almost 30%.<sup>178</sup> The hierarchical structure improved the light harvesting from the material, in addition to providing a greater number of active sites. The second work was also a heterojunction, but with  $Nb_2O_5$  nanotubes ( $Nb_2O_5$ NT/PHI),<sup>84</sup> once nanotubular structures present some advantages like high surface area, a large number of active sites, and especially for photoelectrocatalysis usually better charge separation and transfer,<sup>179–181</sup> and higher density of bulk states than for conventional nanoparticles.<sup>182</sup>  $Nb_2O_5$ NT alone had energy potential enough to perform the ammonia PEC synthesis, however, the synergic effect observed on the heterojunction led to an ammonia generation rate of  $0.156 \text{ mmol L}^{-1} \text{h}^{-1} \text{cm}^{-2}$ , which was about 10-fold higher than just the niobium pentoxide. As Figure 12 shows, the obtained  $Nb_2O_5$ NT/PHI photocathode performed the  $N_2$ RR by a Z-scheme charge transfer, and the improved results can be attributed to PHI favoring  $N_2$  adsorption and activation.

Although there have been relatively few studies on PEC ammonia synthesis using PCN-based catalysts, the environmentally friendly conditions employed in these studies, such as the use of simulated sunlight and low toxicity catalysts, place the obtained photoelectrodes as promising alternatives to the conventional Haber–Bosch process.

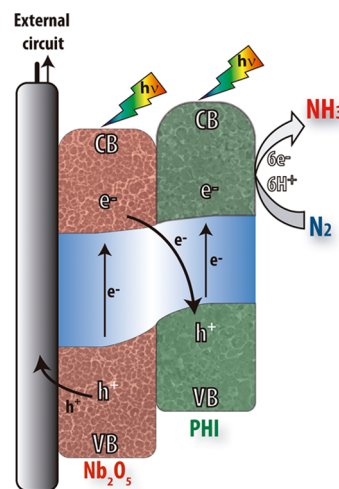


**Figure 12.** Proposed charge transfer mechanism for  $N_2$  reduction over the  $Nb_2O_5$ Nt/PHI Z-scheme. Reproduced with permission from ref 84. Copyright 2023 John Wiley and Sons.

#### 4. CONCLUSION

Carbon nitride materials are highly versatile semiconductors that have a wide range of applications. Anyhow, most of their applications in photoelectrochemistry are focused on water splitting, a sustainable approach for generating high-purity hydrogen owing to advantages such as the availability of a plentiful hydrogen source and utilization of renewable solar energy.

In the matter of biomass upgrading, intergovernmental panels on climate change emphasize the significance of bioenergy with carbon capture and storage in various climate mitigation policy pathways.<sup>183,184</sup> While carbon capture and storage can effectively contribute to achieving net-zero emissions by 2050, it is crucial to address the long-term goal of closing the carbon cycle. Consequently, in the future, there are promising prospects for utilizing biomass, e.g., from waste through photoelectrolysis to generate value-added products like hydrogen and hydrocarbons.

Table 2 provides a summary of the key findings related to other applications beyond water splitting. This versatility of  $C_3N_4$  materials can be attributed mainly to their good chemical stability, allied to the proper design and engineering of the electrodes, by using one or more modifications as discussed in this review, to tune the electrode properties by increasing the light range absorption or specifically for a given substrate adsorption.

Despite all the above exposures, the areas with more room for exploration are the  $CO_2$  and  $N_2$  reduction. As pointed out previously, PCN materials possess various catalytic sites, including graphitic domains, nitrogen, and carbon vacancies, as well as edges that can be even further modified, which provide active sites for the adsorption and activation of  $N_2$  and  $CO_2$  molecules. Depending on a proper modification, e.g., with a cocatalyst, for improving charge transfer processes and enhancing surface reaction kinetics, the overall efficiency of  $N_2$  and  $CO_2$  reduction can be significantly increased.

Given the exceptional properties of PCN, there is great potential for it to play a pivotal role in the development of new and sustainable synthetic methodologies. As a cheap semiconductor, efficient, and easy to obtain,  $C_3N_4$  materials have a huge potential for growth and achieving the industrial scale.

**Table 2. Main Results for PCN-Based Photoelectrodes on Applications beyond Water Splitting**

Photoelectrode	Application	Main results	Source
PCN@Au	Biomass upgrading	Conversion of glycerol to dihydroxyacetone	152
TiO <sub>2</sub> /Ni-PHI	Biomass upgrading	High photocurrent and obtention of formaldehyde and formic acid	153
pim-11PCN@Pt	Biomass upgrading	Gluconate obtention with an enhanced current response	154
PHI	Biomass upgrading	Alcohol reforming under 0 bias	81
PCN	Biomass upgrading	Conversion of benzyl alcohol to respective aldehyde and further to acid	185
ZnO/PCN/MnO <sub>2</sub>	Remediation	Mineralization of methylene blue	134
PCN/MOF(Fe)	Remediation	Degradation of ciprofloxacin	156
n <sub>vac</sub> PCN	Remediation	Degradation of 4-chlorophenol	96
TiO <sub>2</sub> nta/PCnqds	Remediation	Mineralization of rhodamine B	186
PCN	Remediation	Mineralization of phenol	187
PCN/C <sub>paper</sub>	Remediation and energy	Degradation of methylene blue with concomitant hydrogen generation	188
Au/P-PCN	Remediation and sensing	Degradation and sensing of 4-chlorophenol	157
PCN	Sensing	Detection of trace amounts of Cu <sup>2+</sup>	158
Porphyrin-sensitized PCN	Sensing	Glucose sensing in real serum samples	189
PCN/carbon nanohorns	Sensing	Quantitative sensing of arecoline	190
K-PHI	Sensing	Photomemristive sensor with a high-range glucose detection	191
PCN/GO/Aptamer	Sensing	Aptasensing of kanamycin molecules	192
Pcn@pd	CO <sub>2</sub> reduction	Methanol generation with low bias	85
ZnPc/PHI	CO <sub>2</sub> reduction	Methanol generation as a major product	166
PCN photoanode cu cathode	CO <sub>2</sub> reduction	Formic acid generation selectively	193
Co-porphyrin/pcn	CO <sub>2</sub> reduction	Formic acid generation selectively	194
ZnTe/PCN	CO <sub>2</sub> reduction	Ethanol obtention	195
TiO <sub>2</sub> @pcn	CO <sub>2</sub> reduction	CO obtention	196
MoSe <sub>2</sub> @pcn	N <sub>2</sub> reduction	Ammonia rate of 7.7 μmol h <sup>-1</sup> L <sup>-1</sup> cm <sup>-2</sup>	178
Nb <sub>2</sub> O <sub>5</sub> /phi	N <sub>2</sub> reduction	Ammonia rate of 0.156 mmol L <sup>-1</sup> h <sup>-1</sup> cm <sup>-2</sup>	84

For the upcoming years, it is possible to predict, in the first moment, an increase of research of the less explored areas, and further, after achieving a well-established material for a given application (water splitting, CO<sub>2</sub>RR, or N<sub>2</sub>RR), the next step is scaling up. However, this leads to an unsolved question: Is the better option to increase the electrode size or produce arrays of electrodes connected in parallel? At the moment, arrays show as a more feasible alternative, once increasing the size of the photoelectrode results in some loss, due to charge recombination, parasitic ionic paths, and overpotential losses.<sup>197</sup>

## ■ AUTHOR INFORMATION

### Corresponding Author

Sirlon F. Blaskiewicz – Department of Chemistry, Federal University of São Carlos, São Carlos CEP13565-905 São Paulo, Brazil; [orcid.org/0000-0001-6889-5187](https://orcid.org/0000-0001-6889-5187); Email: [sirlonblask@gmail.com](mailto:sirlonblask@gmail.com)

## Authors

Juliana Lucca Francisco – Department of Chemistry, Federal University of São Carlos, São Carlos CEP13565-905 São Paulo, Brazil

Frank Marken – Department of Chemistry, University of Bath, Claverton Down, Bath BA2 7AY, United Kingdom; [orcid.org/0000-0003-3177-4562](https://orcid.org/0000-0003-3177-4562)

Lucia Helena Mascaro – Department of Chemistry, Federal University of São Carlos, São Carlos CEP13565-905 São Paulo, Brazil; [orcid.org/0000-0001-6908-1097](https://orcid.org/0000-0001-6908-1097)

Complete contact information is available at: <https://pubs.acs.org/10.1021/acsaem.3c02623>

## Author Contributions

The manuscript was written through the contributions of all authors. All authors have approved the final version of the manuscript.

## Notes

The authors declare no competing financial interest.

## ■ ACKNOWLEDGMENTS

This work was supported by the São Paulo Research Foundation (FAPESP) (grants number #2018/16401-8 and #2023/11554-9) FAPESP/SHELL (grant number #2017/11986-5), FAPESP/CEPID (grant number #2013/07296-2). The authors also thanks financial support from Coordenação de Aperfeiçoamento de Pessoal de Nível Superior (CAPES), the Conselho Nacional de Pesquisa e Desenvolvimento (CNPq) #406156/2022-0: #311769/2022-5, and the Financiadora de Estudos e Projetos (FINEP) #01.22.0179.00, #01.23.0645.00.

## ■ REFERENCES

- (1) Smalley, R. E. Future Global Energy Prosperity: The Terawatt Challenge. *MRS Bull.* **2005**, *30* (6), 412–417.
- (2) Hamad, S.; Catlow, C. R. A.; Woodley, S. M.; Lago, S.; Mejías, J. A. Structure and Stability of Small TiO<sub>2</sub> Nanoparticles. *J. Phys. Chem. B* **2005**, *109* (33), 15741–15748.
- (3) Levchenko, A. A.; Li, G.; Boerio-Goates, J.; Woodfield, B. F.; Navrotsky, A. TiO<sub>2</sub> Stability Landscape: Polymorphism, Surface Energy, and Bound Water Energetics. *Chem. Mater.* **2006**, *18* (26), 6324–6332.
- (4) Terna, A. D.; Elemike, E. E.; Mbonu, J. I.; Osafire, O. E.; Ezeani, R. O. The Future of Semiconductors Nanoparticles: Synthesis, Properties and Applications. *Mater. Sci. Eng., B* **2021**, *272*, 115363.
- (5) Wang, P.; Liu, Z.; Lin, F.; Zhou, G.; Wu, J.; Duan, W.; Gu, B.-L.; Zhang, S. B. Optimizing Photoelectrochemical Properties of TiO<sub>2</sub> by Chemical Codoping. *Phys. Rev. B* **2010**, *82* (19), 193103.
- (6) Mo, L.-B.; Bai, Y.; Xiang, Q.-Y.; Li, Q.; Wang, J.-O.; Ibrahim, K.; Cao, J.-L. Band Gap Engineering of TiO<sub>2</sub> through Hydrogenation. *Appl. Phys. Lett.* **2014**, *105* (20), 202114 DOI: [10.1063/1.4902445](https://doi.org/10.1063/1.4902445).
- (7) Dette, C.; Pérez-Osorio, M. A.; Kley, C. S.; Punke, P.; Patrick, C. E.; Jacobson, P.; Giustino, F.; Jung, S. J.; Kern, K. TiO<sub>2</sub> Anatase with a Bandgap in the Visible Region. *Nano Lett.* **2014**, *14* (11), 6533–6538.
- (8) Sang, Y.; Liu, H.; Umar, A. Photocatalysis from UV/Vis to Near-Infrared Light: Towards Full Solar-Light Spectrum Activity. *ChemCatChem.* **2015**, *7* (4), 559–573.
- (9) Granata, J. E.; Sites, J. R.; Contreras-Puente, G.; Compaan, A. D. Effect of CdS Thickness on CdS/CdTe Quantum Efficiency [Solar Cells]. In *Conference Record of the Twenty Fifth IEEE Photovoltaic Specialists Conference - 1996*; IEEE, 1996; pp 853–856.
- (10) Yang, W.; Prabhakar, R. R.; Tan, J.; Tilley, S. D.; Moon, J. Strategies for Enhancing the Photocurrent, Photovoltage, and Stability

of Photoelectrodes for Photoelectrochemical Water Splitting. *Chem. Soc. Rev.* **2019**, *48* (19), 4979–5015.

(11) Xu, Y.; Huang, Y.; Zhang, B. Rational Design of Semiconductor-Based Photocatalysts for Advanced Photocatalytic Hydrogen Production: The Case of Cadmium Chalcogenides. *Inorg. Chem. Front.* **2016**, *3* (5), 591–615.

(12) Smith, K. S. Cadmium. In: *Geochemistry. Encyclopedia of Earth Science*. In *Geochemistry. Encyclopedia of Earth Science*; Springer International Publishing: Dordrecht, 1998; pp 50–51.

(13) Qi, X.; Ren, Z.; Cui, Y.; Zhang, J.; Zhang, Y.; Wang, S.; Lin, H. Cadmium Induces Apoptosis by MiR-9–5p Targeting PTEN and Regulates the PI3K/AKT Pathway in the Piglet Adrenal Gland. *Environ. Sci. Pollut. Res.* **2022**, *29* (48), 73001–73010.

(14) Dong, Q.; Mohamad Latiff, N.; Mazánek, V.; Rosli, N. F.; Chia, H. L.; Sofer, Z.; Pumera, M. Triazine- and Heptazine-Based Carbon Nitrides: Toxicity. *ACS Appl. Nano Mater.* **2018**, *1* (9), 4442–4449.

(15) Chng, E. L. K.; Pumera, M. The Toxicity of Graphene Oxides: Dependence on the Oxidative Methods Used. *Chem. - A Eur. J.* **2013**, *19* (25), 8227–8235.

(16) Tian, N.; Huang, H.; Du, X.; Dong, F.; Zhang, Y. Rational Nanostructure Design of Graphitic Carbon Nitride for Photocatalytic Applications. *J. Mater. Chem. A* **2019**, *7* (19), 11584–11612.

(17) Wang, Y.; Liu, L.; Ma, T.; Zhang, Y.; Huang, H. 2D Graphitic Carbon Nitride for Energy Conversion and Storage. *Adv. Funct. Mater.* **2021**, *31* (34), 2102540.

(18) Tripathi, N.; Hills, C. D.; Singh, R. S.; Atkinson, C. J. Biomass Waste Utilisation in Low-Carbon Products: Harnessing a Major Potential Resource. *npj Clim. Atmos. Sci.* **2019**, *2* (1), 35.

(19) Teixeira, I. F.; Barbosa, E. C. M.; Tsang, S. C. E.; Camargo, P. H. C. Carbon Nitrides and Metal Nanoparticles: From Controlled Synthesis to Design Principles for Improved Photocatalysis. *Chem. Soc. Rev.* **2018**, *47* (20), 7783–7817.

(20) Zhao, Z.; Sun, Y.; Dong, F. Graphitic Carbon Nitride Based Nanocomposites: A Review. *Nanoscale* **2015**, *7* (1), 15–37.

(21) Butchosa, C.; Guiglian, P.; Zwijnenburg, M. A. Carbon Nitride Photocatalysts for Water Splitting: A Computational Perspective. *J. Phys. Chem. C* **2014**, *118* (43), 24833–24842.

(22) Wang, X.; Blechert, S.; Antonietti, M. Polymeric Graphitic Carbon Nitride for Heterogeneous Photocatalysis. *ACS Catal.* **2012**, *2* (8), 1596–1606.

(23) Kessler, F. K.; Zheng, Y.; Schwarz, D.; Merschjann, C.; Schnick, W.; Wang, X.; Bojdys, M. J. Functional Carbon Nitride Materials — Design Strategies for Electrochemical Devices. *Nat. Rev. Mater.* **2017**, *2* (6), 17030.

(24) Thomas, A.; Fischer, A.; Goettmann, F.; Antonietti, M.; Müller, J.-O.; Schlögl, R.; Carlsson, J. M. Graphitic Carbon Nitride Materials: Variation of Structure and Morphology and Their Use as Metal-Free Catalysts. *J. Mater. Chem.* **2008**, *18* (41), 4893.

(25) Hwang, S.; Lee, S.; Yu, J.-S. Template-Directed Synthesis of Highly Ordered Nanoporous Graphitic Carbon Nitride through Polymerization of Cyanamide. *Appl. Surf. Sci.* **2007**, *253* (13), 5656–5659.

(26) Kesavan, G.; Sorescu, D. C.; Zeng, Z.; Askari, F.; He, Y.; Rosi, N. L.; Star, A. Optimizing Dicyandiamide Pretreatment Conditions for Enhanced Structure and Electronic Properties of Polymeric Graphitic Carbon Nitride. *J. Mater. Chem. C* **2023**, *11* (42), 14865–14875.

(27) Lotsch, B. V.; Schnick, W. Thermal Conversion of Guanylurea Dicyanamide into Graphitic Carbon Nitride via Prototype CN x Precursors. *Chem. Mater.* **2005**, *17* (15), 3976–3982.

(28) Xu, J.; Chen, T.; Jiang, Q.; Li, Y. Utilization of Environmentally Benign Dicyandiamide as a Precursor for the Synthesis of Ordered Mesoporous Carbon Nitride and Its Application in Base-Catalyzed Reactions. *Chem. - An Asian J.* **2014**, *9* (11), 3269–3277.

(29) Zhang, Y.; Liu, J.; Wu, G.; Chen, W. Porous Graphitic Carbon Nitride Synthesized via Direct Polymerization of Urea for Efficient Sunlight-Driven Photocatalytic Hydrogen Production. *Nanoscale* **2012**, *4* (17), 5300.

(30) Mukhopadhyay, T. K.; Leherte, L.; Datta, A. Molecular Mechanism for the Self-Supported Synthesis of Graphitic Carbon Nitride from Urea Pyrolysis. *J. Phys. Chem. Lett.* **2021**, *12* (5), 1396–1406.

(31) Fang, H.-B.; Luo, Y.; Zheng, Y.-Z.; Ma, W.; Tao, X. Facile Large-Scale Synthesis of Urea-Derived Porous Graphitic Carbon Nitride with Extraordinary Visible-Light Spectrum Photodegradation. *Ind. Eng. Chem. Res.* **2016**, *55* (16), 4506–4514.

(32) Dziubek, K.; Citroni, M.; Fanetti, S.; Cairns, A. B.; Bini, R. Synthesis of High-Quality Crystalline Carbon Nitride Oxide by Selectively Driving the High-Temperature Instability of Urea with Pressure. *J. Phys. Chem. C* **2017**, *121* (36), 19872–19879.

(33) Li, X.; Zhang, J.; Shen, L.; Ma, Y.; Lei, W.; Cui, Q.; Zou, G. Preparation and Characterization of Graphitic Carbon Nitride through Pyrolysis of Melamine. *Appl. Phys. A: Mater. Sci. Process.* **2009**, *94* (2), 387–392.

(34) Liang, Q.; Shao, B.; Tong, S.; Liu, Z.; Tang, L.; Liu, Y.; Cheng, M.; He, Q.; Wu, T.; Pan, Y.; Huang, J.; Peng, Z. Recent Advances of Melamine Self-Assembled Graphitic Carbon Nitride-Based Materials: Design, Synthesis and Application in Energy and Environment. *Chem. Eng. J.* **2021**, *405*, 126951.

(35) Zhai, H.-S.; Cao, L.; Xia, X.-H. Synthesis of Graphitic Carbon Nitride through Pyrolysis of Melamine and Its Electrocatalysis for Oxygen Reduction Reaction. *Chin. Chem. Lett.* **2013**, *24* (2), 103–106.

(36) Wang, J.; Wang, S. A Critical Review on Graphitic Carbon Nitride (g-C<sub>3</sub>N<sub>4</sub>)-Based Materials: Preparation, Modification and Environmental Application. *Coord. Chem. Rev.* **2022**, *453*, 214338.

(37) Hua, S.; Qu, D.; An, L.; Jiang, W.; Wen, Y.; Wang, X.; Sun, Z. Highly Efficient P-Type Cu<sub>3</sub>P/n-Type g-C<sub>3</sub>N<sub>4</sub> Photocatalyst through Z-Scheme Charge Transfer Route. *Appl. Catal. B Environ.* **2019**, *240*, 253–261.

(38) Schwarzer, A.; Saplinova, T.; Kroke, E. Tri-s-Triazines (s-Heptazines)—From a “Mystery Molecule” to Industrially Relevant Carbon Nitride Materials. *Coord. Chem. Rev.* **2013**, *257* (13–14), 2032–2062.

(39) Cao, S.; Low, J.; Yu, J.; Jaroniec, M. Polymeric Photocatalysts Based on Graphitic Carbon Nitride. *Adv. Mater.* **2015**, *27* (13), 2150–2176.

(40) Niu, P.; Yin, L.-C.; Yang, Y.-Q.; Liu, G.; Cheng, H.-M. Increasing the Visible Light Absorption of Graphitic Carbon Nitride (Melon) Photocatalysts by Homogeneous Self-Modification with Nitrogen Vacancies. *Adv. Mater.* **2014**, *26* (47), 8046–8052.

(41) Chen, Z.; Savateev, A.; Pronkin, S.; Papaefthimiou, V.; Wolff, C.; Willinger, M. G.; Willinger, E.; Neher, D.; Antonietti, M.; Dontsova, D. The Easier the Better” Preparation of Efficient Photocatalysts-Metastable Poly(Heptazine Imide) Salts. *Adv. Mater.* **2017**, *29* (32), 1700555.

(42) Bojdys, M. J.; Müller, J.; Antonietti, M.; Thomas, A. Ionothermal Synthesis of Crystalline, Condensed, Graphitic Carbon Nitride. *Chem. - A Eur. J.* **2008**, *14* (27), 8177–8182.

(43) Algara-Siller, G.; Severin, N.; Chong, S. Y.; Björkman, T.; Palgrave, R. G.; Laybourn, A.; Antonietti, M.; Khimyak, Y. Z.; Krasheninnikov, A. V.; Rabe, J. P.; Kaiser, U.; Cooper, A. I.; Thomas, A.; Bojdys, M. J. Triazine-Based Graphitic Carbon Nitride: A Two-Dimensional Semiconductor. *Angew. Chemie Int. Ed.* **2014**, *53* (29), 7450–7455.

(44) Colombari, F. M.; da Silva, M. A. R.; Homsí, M. S.; de Souza, B. R. L.; Araujo, M.; Francisco, J. L.; da Silva, G. T. S. T.; Silva, I. F.; de Moura, A. F.; Teixeira, I. F. Graphitic Carbon Nitrides as Platforms for Single-Atom Photocatalysis. *Faraday Discuss.* **2021**, *227*, 306–320.

(45) Chen, Z.; Savateev, A.; Pronkin, S.; Papaefthimiou, V.; Wolff, C.; Willinger, M. G.; Willinger, E.; Neher, D.; Antonietti, M.; Dontsova, D. The Easier the Better” Preparation of Efficient Photocatalysts-Metastable Poly(Heptazine Imide) Salts. *Adv. Mater.* **2017**, *29* (32), 1700555.

(46) Savateev, A.; Kurpil, B.; Mishchenko, A.; Zhang, G.; Antonietti, M. A “Waiting” Carbon Nitride Radical Anion: A Charge Storage Material and Key Intermediate in Direct C-H Thiolation of

Methylarenes Using Elemental Sulfur as the “S”-Source. *Chem. Sci.* **2018**, *9* (14), 3584–3591.

(47) Krivtsov, I.; Mitoraj, D.; Adler, C.; Ilkaeva, M.; Sardo, M.; Mafra, L.; Neumann, C.; Turchanin, A.; Li, C.; Dietzek, B.; Leiter, R.; Biskupek, J.; Kaiser, U.; Im, C.; Kirchhoff, B.; Jacob, T.; Beranek, R. Water-Soluble Polymeric Carbon Nitride Colloidal Nanoparticles for Highly Selective Quasi-Homogeneous Photocatalysis. *Angew. Chem.* **2020**, *132* (1), 495–503.

(48) Lau, V. W.; Klose, D.; Kasap, H.; Podjaski, F.; Pigní, M.; Reisner, E.; Jeschke, G.; Lotsch, B. V. Dark Photocatalysis: Storage of Solar Energy in Carbon Nitride for Time-Delayed Hydrogen Generation. *Angew. Chemie Int. Ed.* **2017**, *56* (2), 510–514.

(49) Adler, C.; Selim, S.; Krivtsov, I.; Li, C.; Mitoraj, D.; Dietzek, B.; Durrant, J. R.; Beranek, R. Photodoping and Fast Charge Extraction in Ionic Carbon Nitride Photoanodes. *Adv. Funct. Mater.* **2021**, *31* (45), 2105369.

(50) Ajiboye, T. O.; Kuvarega, A. T.; Onwudiwe, D. C. Graphitic Carbon Nitride-Based Catalysts and Their Applications: A Review. *Nano-Structures & Nano-Objects* **2020**, *24*, 100577.

(51) Shi, J.; Tai, M.; Hou, J.; Qiao, Y.; Liu, C.; Zhou, T.; Wang, L.; Hu, B. Intramolecular D-A Structure and n- $\pi^*$  Transition Co-Promoted Photodegradation Activity of Carbon Nitride: Performance, Mechanism and Toxicity Insight. *Chem. Eng. J.* **2023**, *456*, 141029.

(52) Zhou, T.; Shi, J.; Li, G.; Liu, B.; Hu, B.; Che, G.; Liu, C.; Wang, L.; Yan, L. Advancing N- $\pi^*$  Electron Transition of Carbon Nitride via Distorted Structure and Nitrogen Heterocycle for Efficient Photodegradation: Performance, Mechanism and Toxicity Insight. *J. Colloid Interface Sci.* **2023**, *632*, 285–298.

(53) Zhao, G.-Q.; Zou, J.; Hu, J.; Long, X.; Jiao, F.-P. A Critical Review on Graphitic Carbon Nitride (g-C<sub>3</sub>N<sub>4</sub>)-Based Composites for Environmental Remediation. *Sep. Purif. Technol.* **2021**, *279*, 119769.

(54) Wang, X.; Maeda, K.; Thomas, A.; Takanabe, K.; Xin, G.; Carlsson, J. M.; Domen, K.; Antonietti, M. A Metal-Free Polymeric Photocatalyst for Hydrogen Production from Water under Visible Light. *Nat. Mater.* **2009**, *8* (1), 76–80.

(55) Xiong, W.; Huang, F.; Zhang, R.-Q. Recent Developments in Carbon Nitride Based Films for Photoelectrochemical Water Splitting. *Sustain. Energy Fuels* **2020**, *4* (2), 485–503.

(56) Wang, L.; Si, W.; Tong, Y.; Hou, F.; Pergolesi, D.; Hou, J.; Lippert, T.; Dou, S. X.; Liang, J. Graphitic Carbon Nitride (G-C<sub>3</sub>N<sub>4</sub>)-based Nanosized Heteroarrays: Promising Materials for Photoelectrochemical Water Splitting. *Carbon Energy* **2020**, *2* (2), 223–250.

(57) Volokh, M.; Peng, G.; Barrio, J.; Shalom, M. Carbon Nitride Materials for Water Splitting Photoelectrochemical Cells. *Angew. Chemie Int. Ed.* **2019**, *58* (19), 6138–6151.

(58) Liu, J.; Fu, W.; Liao, Y.; Fan, J.; Xiang, Q. Recent Advances in Crystalline Carbon Nitride for Photocatalysis. *J. Mater. Sci. Technol.* **2021**, *91*, 224–240.

(59) Blaskiewicz, S. F.; Mascaro, L. H.; Zhao, Y.; Marken, F. Semiconductor Photoelectroanalysis and Photobioelectroanalysis: A Perspective. *TrAC - Trends Anal. Chem.* **2021**, *135*, 116154.

(60) Merschjann, C.; Tschierlei, S.; Tyborski, T.; Kailasam, K.; Orthmann, S.; Hollmann, D.; Schedel-Niedrig, T.; Thomas, A.; Lochbrunner, S. Complementing Graphenes: 1D Interplanar Charge Transport in Polymeric Graphitic Carbon Nitrides. *Adv. Mater.* **2015**, *27* (48), 7993–7999.

(61) Noda, Y.; Merschjann, C.; Tarábek, J.; Amsalem, P.; Koch, N.; Bojdys, M. J. Directional Charge Transport in Layered Two-Dimensional Triazine-Based Graphitic Carbon Nitride. *Angew. Chemie Int. Ed.* **2019**, *58* (28), 9394–9398.

(62) Heeney, M.; Bailey, C.; Genevicius, K.; Shkunov, M.; Sparrowe, D.; Tierney, S.; McCulloch, I. Stable Polythiophene Semiconductors Incorporating Thieno[2,3-*b*]Thiophene. *J. Am. Chem. Soc.* **2005**, *127* (4), 1078–1079.

(63) Venugopal, G.; Krishnamoorthy, K.; Mohan, R.; Kim, S.-J. An Investigation of the Electrical Transport Properties of Graphene-Oxide Thin Films. *Mater. Chem. Phys.* **2012**, *132* (1), 29–33.

(64) Giannini, S.; Blumberger, J. Charge Transport in Organic Semiconductors: The Perspective from Nonadiabatic Molecular Dynamics. *Acc. Chem. Res.* **2022**, *55* (6), 819–830.

(65) Fratini, S.; Nikolka, M.; Sallee, A.; Schweicher, G.; Siringhaus, H. Charge Transport in High-Mobility Conjugated Polymers and Molecular Semiconductors. *Nat. Mater.* **2020**, *19* (5), 491–502.

(66) Siringhaus, H.; Sakanoue, T.; Chang, J. Charge-transport Physics of High-mobility Molecular Semiconductors. *Phys. status solidi* **2012**, *249* (9), 1655–1676.

(67) Singh, B.; Singh, J.; Kaur, J.; Moudgil, R. K.; Tripathi, S. K. Investigations of the Drift Mobility of Carriers and Density of States in Nanocrystalline CdS Thin Films. *Phys. B Condens. Matter* **2016**, *490*, 49–56.

(68) Lee, J.-S.; Kovalenko, M. V.; Huang, J.; Chung, D. S.; Talapin, D. V. Band-like Transport, High Electron Mobility and High Photoconductivity in All-Inorganic Nanocrystal Arrays. *Nano-technol.* **2011**, *6* (6), 348–352.

(69) Tiwana, P.; Docampo, P.; Johnston, M. B.; Snaith, H. J.; Herz, L. M. Electron Mobility and Injection Dynamics in Mesoporous ZnO, SnO<sub>2</sub>, and TiO<sub>2</sub> Films Used in Dye-Sensitized Solar Cells. *ACS Nano* **2011**, *5* (6), 5158–5166.

(70) Chandiran, A. K.; Abdi-Jalebi, M.; Nazeeruddin, M. K.; Grätzel, M. Analysis of Electron Transfer Properties of ZnO and TiO<sub>2</sub> Photoanodes for Dye-Sensitized Solar Cells. *ACS Nano* **2014**, *8* (3), 2261–2268.

(71) Ai, M.; Pan, L.; Chen, Y.; Shi, C.; Huang, Z.-F.; Zhang, X.; Zou, J.-J. Atomic Symmetry Alteration in Carbon Nitride to Modulate Charge Distribution for Efficient Photocatalysis. *J. Catal.* **2023**, *418*, 22–30.

(72) Wu, B.; Zhang, L.; Jiang, B.; Li, Q.; Tian, C.; Xie, Y.; Li, W.; Fu, H. Ultrathin Porous Carbon Nitride Bundles with an Adjustable Energy Band Structure toward Simultaneous Solar Photocatalytic Water Splitting and Selective Phenylcarbinol Oxidation. *Angew. Chemie Int. Ed.* **2021**, *60* (9), 4815–4822.

(73) Liang, Q.; Li, Z.; Huang, Z.; Kang, F.; Yang, Q. Holey Graphitic Carbon Nitride Nanosheets with Carbon Vacancies for Highly Improved Photocatalytic Hydrogen Production. *Adv. Funct. Mater.* **2015**, *25* (44), 6885–6892.

(74) Hankin, A.; Bedoya-Lora, F. E.; Alexander, J. C.; Regoutz, A.; Kelsall, G. H. Flat Band Potential Determination: Avoiding the Pitfalls. *J. Mater. Chem. A* **2019**, *7* (45), 26162–26176.

(75) Koshevoy, E.; Gribov, E.; Polskikh, D.; Lyulyukin, M.; Solovyeva, M.; Cherepanova, S.; Kozlov, D.; Selishchev, D. Photoelectrochemical Methods for the Determination of the Flat-Band Potential in Semiconducting Photocatalysts: A Comparison Study. *Langmuir* **2023**, *39* (38), 13466–13480.

(76) Wojtyła, S.; Śpiewak, K.; Baran, T. Doped Graphitic Carbon Nitride: Insights from Spectroscopy and Electrochemistry. *J. Inorg. Organomet. Polym. Mater.* **2020**, *30* (9), 3418–3428.

(77) Capilli, G.; Costamagna, M.; Sordello, F.; Minero, C. Synthesis, Characterization and Photocatalytic Performance of p-Type Carbon Nitride. *Appl. Catal. B Environ.* **2019**, *242*, 121–131.

(78) Peraus, P. On Electronegativity of Graphitic Carbon Nitride. *Carbon N. Y.* **2021**, *172*, 729–732.

(79) Sivula, K. Mott-Schottky Analysis of Photoelectrodes: Sanity Checks Are Needed. *ACS Energy Lett.* **2021**, *6* (7), 2549–2551.

(80) Chu, S.; Wang, Y.; Guo, Y.; Feng, J.; Wang, C.; Luo, W.; Fan, X.; Zou, Z. Band Structure Engineering of Carbon Nitride: In Search of a Polymer Photocatalyst with High Photooxidation Property. *ACS Catal.* **2013**, *3* (5), 912–919.

(81) Adler, C.; Krivtsov, I.; Mitoraj, D.; dos Santos-Gómez, L.; García-Granda, S.; Neumann, C.; Kund, J.; Kranz, C.; Mizaikoff, B.; Turchanin, A.; Beranek, R. Sol-Gel Processing of Water-Soluble Carbon Nitride Enables High-Performance Photoanodes\*\*. *ChemSusChem* **2021**, *14* (10), 2170–2179.

(82) Liu, N.; Li, T.; Zhao, Z.; Liu, J.; Luo, X.; Yuan, X.; Luo, K.; He, J.; Yu, D.; Zhao, Y. From Triazine to Heptazine: Origin of Graphitic Carbon Nitride as a Photocatalyst. *ACS Omega* **2020**, *5* (21), 12557–12567.

- (83) Gu, Q.; Gong, X.; Jia, Q.; Liu, J.; Gao, Z.; Wang, X.; Long, J.; Xue, C. Compact Carbon Nitride Based Copolymer Films with Controllable Thickness for Photoelectrochemical Water Splitting. *J. Mater. Chem. A* **2017**, *5* (36), 19062–19071.
- (84) Blaskiewicz, S. F.; Freitas Teixeira, I.; Mascaro, L. H.; Ferreira de Brito, J. Direct Z-scheme among Niobium Pentoxide and Poly(Heptazine Imide) for NH<sub>3</sub> Photoelectrosynthesis under Ambient Conditions. *ChemCatChem*. **2023**, e202201610.
- (85) Xu, Y.; Wang, S.; Yang, J.; Han, B.; Nie, R.; Wang, J.; Dong, Y.; Yu, X.; Wang, J.; Jing, H. Highly Efficient Photoelectrocatalytic Reduction of CO<sub>2</sub> on the Ti<sub>3</sub>C<sub>2</sub>/g-C<sub>3</sub>N<sub>4</sub> Heterojunction with Rich Ti<sup>3+</sup> and Pyri-N Species. *J. Mater. Chem. A* **2018**, *6* (31), 15213–15220.
- (86) Kumar, A.; Raizada, P.; Hosseini-Bandegharai, A.; Thakur, V. K.; Nguyen, V.-H.; Singh, P. C., N-Vacancy Defect Engineered Polymeric Carbon Nitride towards Photocatalysis: Viewpoints and Challenges. *J. Mater. Chem. A* **2021**, *9* (1), 111–153.
- (87) Kubota, J.; Domen, K. Photocatalytic Water Splitting Using Oxynitride and Nitride Semiconductor Powders for Production of Solar Hydrogen. *Interface Mag.* **2013**, *22* (2), 57–62.
- (88) Huang, X.; Gu, W.; Ma, Y.; Liu, D.; Ding, N.; Zhou, L.; Lei, J.; Wang, L.; Zhang, J. Recent Advances of Doped Graphite Carbon Nitride for Photocatalytic Reduction of CO<sub>2</sub>: A Review. *Res. Chem. Intermed.* **2020**, *46* (12), 5133–5164.
- (89) Vu, M.-H.; Sakar, M.; Do, T.-O. Insights into the Recent Progress and Advanced Materials for Photocatalytic Nitrogen Fixation for Ammonia (NH<sub>3</sub>) Production. *Catalysts* **2018**, *8* (12), 621.
- (90) Huang, M.; Zhao, Y.-L.; Xiong, W.; Kershaw, S. V.; Yu, Y.; Li, W.; Dudka, T.; Zhang, R.-Q. Collaborative Enhancement of Photon Harvesting and Charge Carrier Dynamics in Carbon Nitride Photoelectrode. *Appl. Catal. B Environ.* **2018**, *237*, 783–790.
- (91) Kumar, P.; Thakur, U. K.; Alam, K.; Kar, P.; Kisslinger, R.; Zeng, S.; Patel, S.; Shankar, K. Arrays of TiO<sub>2</sub> Nanorods Embedded with Fluorine Doped Carbon Nitride Quantum Dots (CNFQDs) for Visible Light Driven Water Splitting. *Carbon N. Y.* **2018**, *137*, 174–187.
- (92) Fang, Y.; Li, X.; Wang, Y.; Giordano, C.; Wang, X. Gradient Sulfur Doping along Polymeric Carbon Nitride Films as Visible Light Photoanodes for the Enhanced Water Oxidation. *Appl. Catal. B Environ.* **2020**, *268*, 118398.
- (93) Putri, L. K.; Ng, B.-J.; Ong, W.-J.; Lee, H. W.; Chang, W. S.; Chai, S.-P. Engineering Nanoscale p-n Junction via the Synergetic Dual-Doping of p-Type Boron-Doped Graphene Hybridized with n-Type Oxygen-Doped Carbon Nitride for Enhanced Photocatalytic Hydrogen Evolution. *J. Mater. Chem. A* **2018**, *6* (7), 3181–3194.
- (94) Huang, M.; Wang, H.; Li, W.; Zhao, Y.-L.; Zhang, R.-Q. In Situ Textured Carbon Nitride Photoanodes with Enhanced Photoelectrochemical Activity by Band-Gap State Modulation. *J. Mater. Chem. A* **2020**, *8* (45), 24005–24012.
- (95) Lin, F.; Wang, T.; Ren, Z.; Cai, X.; Wang, Y.; Chen, J.; Wang, J.; Zang, S.; Mao, F.; Lv, L. Central Nitrogen Vacancies in Polymeric Carbon Nitride for Boosted Photocatalytic H<sub>2</sub>O<sub>2</sub> Production. *J. Colloid Interface Sci.* **2023**, *636*, 223–229.
- (96) Hou, Y.; Yang, J.; Lei, C.; Yang, B.; Li, Z.; Xie, Y.; Zhang, X.; Lei, L.; Chen, J. Nitrogen Vacancy Structure Driven Photoelectrocatalytic Degradation of 4-Chlorophenol Using Porous Graphitic Carbon Nitride Nanosheets. *ACS Sustain. Chem. Eng.* **2018**, *6* (5), 6497–6506.
- (97) Cao, J.; Nie, W.; Huang, L.; Ding, Y.; Lv, K.; Tang, H. Photocatalytic Activation of Sulfite by Nitrogen Vacancy Modified Graphitic Carbon Nitride for Efficient Degradation of Carbamazepine. *Appl. Catal. B Environ.* **2019**, *241*, 18–27.
- (98) Bian, J.; Xi, L.; Li, J.; Xiong, Z.; Huang, C.; Lange, K. M.; Tang, J.; Shalom, M.; Zhang, R.-Q. C = C  $\pi$  Bond Modified Graphitic Carbon Nitride Films for Enhanced Photoelectrochemical Cell Performance. *Chem. - An Asian J.* **2017**, *12* (9), 1005–1012.
- (99) Peng, G.; Volokh, M.; Tzadikov, J.; Sun, J.; Shalom, M. Carbon Nitride/Reduced Graphene Oxide Film with Enhanced Electron Diffusion Length: An Efficient Photo-Electrochemical Cell for Hydrogen Generation. *Adv. Energy Mater.* **2018**, *8* (23), 1800566.
- (100) Blaskiewicz, S. F.; Santos, H. L. S.; Teixeira, I. F.; Bott-Neto, J. L.; Fernández, P. S.; Mascaro, L. H. Nickel-Modified Polymeric Carbon Nitride for Improving TiO<sub>2</sub>-Based Photoanode: Photoelectrocatalytic Evaluation and Mechanistical Insights. *Mater. Today Nano* **2022**, *18*, 100192.
- (101) Wang, Y.; Xu, Y.; Wang, Y.; Qin, H.; Li, X.; Zuo, Y.; Kang, S.; Cui, L. Synthesis of Mo-Doped Graphitic Carbon Nitride Catalysts and Their Photocatalytic Activity in the Reduction of CO<sub>2</sub> with H<sub>2</sub>O. *Catal. Commun.* **2016**, *74*, 75–79.
- (102) Karjule, N.; Barrio, J.; Xing, L.; Volokh, M.; Shalom, M. Highly Efficient Polymeric Carbon Nitride Photoanode with Excellent Electron Diffusion Length and Hole Extraction Properties. *Nano Lett.* **2020**, *20* (6), 4618–4624.
- (103) Niu, P.; Zhang, L.; Liu, G.; Cheng, H.-M. Graphene-Like Carbon Nitride Nanosheets for Improved Photocatalytic Activities. *Adv. Funct. Mater.* **2012**, *22* (22), 4763–4770.
- (104) Xu, W.; Lai, S.; Pillai, S. C.; Chu, W.; Hu, Y.; Jiang, X.; Fu, M.; Wu, X.; Li, F.; Wang, H. Visible Light Photocatalytic Degradation of Tetracycline with Porous Ag/Graphite Carbon Nitride Plasmonic Composite: Degradation Pathways and Mechanism. *J. Colloid Interface Sci.* **2020**, *574*, 110–121.
- (105) Dai, H.; Zhang, S.; Li, Y.; Lin, Y. Excellent Graphitic Carbon Nitride Nanosheets-Based Photoelectrochemical Platform Motivated by Schottky Barrier and LSPR Effect and Its Sensing Application. *Analyst* **2015**, *140* (10), 3514–3520.
- (106) Dong, Y.-X.; Cao, J.-T.; Wang, B.; Ma, S.-H.; Liu, Y.-M. Exciton-Plasmon Interactions between CdS@g-C<sub>3</sub>N<sub>4</sub> Heterojunction and Au@Ag Nanoparticles Coupled with DNAase-Triggered Signal Amplification: Toward Highly Sensitive Photoelectrochemical Bioanalysis of MicroRNA. *ACS Sustain. Chem. Eng.* **2017**, *5* (11), 10840–10848.
- (107) Zhu, J.-N.; Zhu, X.-Q.; Cheng, F.-F.; Li, P.; Wang, F.; Xiao, Y.-W.; Xiong, W.-W. Preparing Copper Doped Carbon Nitride from Melamine Templated Crystalline Copper Chloride for Fenton-like Catalysis. *Appl. Catal. B Environ.* **2019**, *256*, 117830.
- (108) Murugan, C.; Ranjithkumar, K.; Pandikumar, A. Interfacial Charge Dynamics in Type-II Heterostructured Sulfur Doped-Graphitic Carbon Nitride/Bismuth Tungstate as Competent Photoelectrocatalytic Water Splitting Photoanode. *J. Colloid Interface Sci.* **2021**, *602*, 437–451.
- (109) Wan, X.; Yu, W.; Niu, H.; Wang, X.; Zhang, Z.; Guo, Y. Revealing the Oxygen Reduction/Evolution Reaction Activity Origin of Carbon-Nitride-Related Single-Atom Catalysts: Quantum Chemistry in Artificial Intelligence. *Chem. Eng. J.* **2022**, *440*, 135946.
- (110) Zhang, J.; Zhang, M.; Lin, S.; Fu, X.; Wang, X. Molecular Doping of Carbon Nitride Photocatalysts with Tunable Bandgap and Enhanced Activity. *J. Catal.* **2014**, *310*, 24–30.
- (111) Bian, J.; Xi, L.; Huang, C.; Lange, K. M.; Zhang, R.-Q.; Shalom, M. Efficiency Enhancement of Carbon Nitride Photoelectrochemical Cells via Tailored Monomers Design. *Adv. Energy Mater.* **2016**, *6* (12), 1600263.
- (112) Barrio, J.; Lin, L.; Amo-Ochoa, P.; Tzadikov, J.; Peng, G.; Sun, J.; Zamora, F.; Wang, X.; Shalom, M. Unprecedented Centimeter-Long Carbon Nitride Needles: Synthesis, Characterization and Applications. *Small* **2018**, *14* (21), 1800633.
- (113) Wei, X.; Liu, X.; Liu, H.; Yang, S.; Zeng, H.; Meng, F.; Lei, X.; Liu, J. Exfoliated Graphitic Carbon Nitride Self-Recognizing CH<sub>3</sub>NH<sub>3</sub>PbI<sub>3</sub> Grain Boundaries by Hydrogen Bonding Interaction for Improved Perovskite Solar Cells. *Sol. Energy* **2019**, *181*, 161–168.
- (114) Peng, G.; Xing, L.; Barrio, J.; Volokh, M.; Shalom, M. A General Synthesis of Porous Carbon Nitride Films with Tunable Surface Area and Photophysical Properties. *Angew. Chemie Int. Ed.* **2018**, *57* (5), 1186–1192.
- (115) Xie, X.; Fan, X.; Huang, X.; Wang, T.; He, J. In Situ Growth of Graphitic Carbon Nitride Films on Transparent Conducting Substrates via a Solvothermal Route for Photoelectrochemical Performance. *RSC Adv.* **2016**, *6* (12), 9916–9922.

- (116) Muhl, S.; Méndez, J. M. A Review of the Preparation of Carbon Nitride Films. *Diam. Relat. Mater.* **1999**, *8* (10), 1809–1830.
- (117) Pawar, R. C.; Pyo, Y.; Ahn, S. H.; Lee, C. S. Photoelectrochemical Properties and Photodegradation of Organic Pollutants Using Hematite Hybrids Modified by Gold Nanoparticles and Graphitic Carbon Nitride. *Appl. Catal. B Environ.* **2015**, *176–177*, 654–666.
- (118) Wang, Y.; Sun, J.; Li, J.; Zhao, X. Electrospinning Preparation of Nanostructured G-C 3 N 4 /BiVO 4 Composite Films with an Enhanced Photoelectrochemical Performance. *Langmuir* **2017**, *33* (19), 4694–4701.
- (119) Schleuning, M.; Ahmet, I. Y.; van de Krol, R.; May, M. M. The Role of Selective Contacts and Built-in Field for Charge Separation and Transport in Photoelectrochemical Devices. *Sustain. Energy Fuels* **2022**, *6* (16), 3701–3716.
- (120) Ruan, Q.; Luo, W.; Xie, J.; Wang, Y.; Liu, X.; Bai, Z.; Carmalt, C. J.; Tang, J. A Nanojunction Polymer Photoelectrode for Efficient Charge Transport and Separation. *Angew. Chem.* **2017**, *129* (28), 8333–8337.
- (121) Thakur, A.; Ghosh, D.; Devi, P.; Kim, K.-H.; Kumar, P. Current Progress and Challenges in Photoelectrode Materials for the Production of Hydrogen. *Chem. Eng. J.* **2020**, *397*, 125415.
- (122) Zhang, Y.; Antonietti, M. Photocurrent Generation by Polymeric Carbon Nitride Solids: An Initial Step towards a Novel Photovoltaic System. *Chem. - An Asian J.* **2010**, *5*, 1307.
- (123) Kaur, N.; Ghosh, A.; Ahmad, M.; Sharma, D.; Singh, R.; Mehta, B. R. Increased Visible Light Absorption and Charge Separation in 2D-3D In<sub>2</sub>S<sub>3</sub>-ZnO Heterojunctions for Enhanced Photoelectrochemical Water Splitting. *J. Alloys Compd.* **2022**, *903*, 164007.
- (124) Jeon, T. H.; Park, C.; Kang, U.; Moon, G.; Kim, W.; Park, H.; Choi, W. Photoelectrochemical Water Oxidation Using Hematite Modified with Metal-Incorporated Graphitic Carbon Nitride Film as a Surface Passivation and Hole Transfer Overlayer. *Appl. Catal. B Environ.* **2024**, *340*, 123167.
- (125) Karjule, N.; Singh, C.; Barrio, J.; Tzadikov, J.; Liberman, I.; Volokh, M.; Palomares, E.; Hod, I.; Shalom, M. Carbon Nitride-Based Photoanode with Enhanced Photostability and Water Oxidation Kinetics. *Adv. Funct. Mater.* **2021**, *31* (25), 2101724.
- (126) Bledowski, M.; Wang, L.; Ramakrishnan, A.; Khavryuchenko, O. V.; Khavryuchenko, V. D.; Ricci, P. C.; Strunk, J.; Cremer, T.; Kolbeck, C.; Beranek, R. Visible-Light Photocurrent Response of TiO<sub>2</sub>-Polyheptazine Hybrids: Evidence for Interfacial Charge-Transfer Absorption. *Phys. Chem. Chem. Phys.* **2011**, *13* (48), 21511.
- (127) Bledowski, M.; Wang, L.; Ramakrishnan, A.; Bétard, A.; Khavryuchenko, O. V.; Beranek, R. Visible-Light Photooxidation of Water to Oxygen at Hybrid TiO<sub>2</sub>-Polyheptazine Photoanodes with Photodeposited Co-Pi (CoO<sub>x</sub>) Cocatalyst. *ChemPhysChem* **2012**, *13* (12), 3018–3024.
- (128) Braun, H.; Mitoraj, D.; Kuncewicz, J.; Hellmann, A.; Elnagar, M. M.; Bansmann, J.; Kranz, C.; Jacob, T.; Macyk, W.; Beranek, R. Polymeric Carbon Nitride-Based Photocathodes for Visible Light-Driven Selective Reduction of Oxygen to Hydrogen Peroxide. *Appl. Catal. A Gen.* **2023**, *660*, 119173.
- (129) Fan, X.; Wang, T.; Gao, B.; Gong, H.; Xue, H.; Guo, H.; Song, L.; Xia, W.; Huang, X.; He, J. Preparation of the TiO<sub>2</sub> /Graphitic Carbon Nitride Core-Shell Array as a Photoanode for Efficient Photoelectrochemical Water Splitting. *Langmuir* **2016**, *32* (50), 13322–13332.
- (130) Zhou, X.; Peng, F.; Wang, H.; Yu, H.; Fang, Y. Carbon Nitride Polymer Sensitized TiO<sub>2</sub> Nanotube Arrays with Enhanced Visible Light Photoelectrochemical and Photocatalytic Performance. *Chem. Commun.* **2011**, *47* (37), 10323.
- (131) Su, J.; Geng, P.; Li, X.; Zhao, Q.; Quan, X.; Chen, G. Novel Phosphorus Doped Carbon Nitride Modified TiO<sub>2</sub> Nanotube Arrays with Improved Photoelectrochemical Performance. *Nanoscale* **2015**, *7* (39), 16282–16289.
- (132) Alberio, J.; Barea, E. M.; Xu, J.; Mora-Seró, I.; Garcia, H.; Shalom, M. Toward Efficient Carbon Nitride Photoelectrochemical Cells: Understanding Charge Transfer Processes. *Adv. Mater. Interfaces* **2017**, *4* (1), 1600265.
- (133) Khavryuchenko, O. V.; Wang, L.; Mitoraj, D.; Peslherbe, G. H.; Beranek, R. Enabling Visible-Light Water Photooxidation by Coordinative Incorporation of Co(II/III) Cocatalytic Sites into Organic-Inorganic Hybrids: Quantum Chemical Modeling and Photoelectrochemical Performance. *J. Coord. Chem.* **2015**, *68* (17–18), 3317–3327.
- (134) He, S.; Xiao, K.; Chen, X.-Z.; Li, T.; Ouyang, T.; Wang, Z.; Guo, M.-L.; Liu, Z.-Q. Enhanced Photoelectrocatalytic Activity of Direct Z-Scheme Porous Amorphous Carbon Nitride/Manganese Dioxide Nanorod Arrays. *J. Colloid Interface Sci.* **2019**, *557*, 644–654.
- (135) Wang, B.; Yu, H.; Quan, X.; Chen, S. Ultra-Thin g-C<sub>3</sub>N<sub>4</sub> Nanosheets Wrapped Silicon Nanowire Array for Improved Chemical Stability and Enhanced Photoresponse. *Mater. Res. Bull.* **2014**, *59*, 179–184.
- (136) Sun, M.; Chen, Z.; Jiang, X.; Feng, C.; Zeng, R. Optimized Preparation of Co-Pi Decorated g-C<sub>3</sub>N<sub>4</sub>@ZnO Shell-Core Nanorod Array for Its Improved Photoelectrochemical Performance and Stability. *J. Alloys Compd.* **2019**, *780*, 540–551.
- (137) Yang, F.; Kuznietsov, V.; Lublow, M.; Merschjann, C.; Steigert, A.; Klaer, J.; Thomas, A.; Schedel-Niedrig, T. Solar Hydrogen Evolution Using Metal-Free Photocatalytic Polymeric Carbon Nitride/CuInS<sub>2</sub> Composites as Photocathodes. *J. Mater. Chem. A* **2013**, *6407*.
- (138) Liu, Y.; Su, F.-Y.; Yu, Y.-X.; Zhang, W.-D. Nano G-C<sub>3</sub>N<sub>4</sub>Modified Ti-Fe<sub>2</sub>O<sub>3</sub> Vertically Arrays for Efficient Photoelectrochemical Generation of Hydrogen under Visible Light. *Int. J. Hydrogen Energy* **2016**, *41* (18), 7270–7279.
- (139) Wang, Z.; Zou, G.; Feng, C.; Ma, Y.; Wang, X.; Bi, Y. Novel Composites of Graphitic Carbon Nitride and NiO Nanosheet Arrays as Effective Photocathodes with Enhanced Photocurrent Performances. *RSC Adv.* **2016**, *6* (86), 83350–83355.
- (140) Mary Rajaiitha, P.; Shamsa, K.; Murugan, C.; Bhojanaa, K. B.; Ravichandran, S.; Jothivenkatachalam, K.; Pandikumar, A. Graphitic Carbon Nitride Nanoplatelets Incorporated Titania Based Type-II Heterostructure and Its Enhanced Performance in Photoelectrocatalytic Water Splitting. *SN Appl. Sci.* **2020**, *2* (4), 572.
- (141) Wei, X.; Jiang, H.; Liu, Z. Liquid-Based Growth of Polymeric Carbon Nitride Films and Their Extraordinary Photoelectrocatalytic Activity. *RSC Adv.* **2016**, *6* (84), 81372–81377.
- (142) Jing, L.; Ong, W.-J.; Zhang, R.; Pickwell-MacPherson, E.; Yu, J. C. Graphitic Carbon Nitride Nanosheet Wrapped Mesoporous Titanium Dioxide for Enhanced Photoelectrocatalytic Water Splitting. *Catal. Today* **2018**, *315*, 103–109.
- (143) Zhan, F.; Xie, R.; Li, W.; Li, J.; Yang, Y.; Li, Y.; Chen, Q. In Situ Synthesis of G-C 3 N 4 /WO 3 Heterojunction Plates Array Films with Enhanced Photoelectrochemical Performance. *RSC Adv.* **2015**, *5* (85), 69753–69760.
- (144) Li, Y.; Wei, X.; Li, H.; Wang, R.; Feng, J.; Yun, H.; Zhou, A. Fabrication of Inorganic-Organic Core-Shell Heterostructure: Novel CdS@g-C 3 N 4 Nanorod Arrays for Photoelectrochemical Hydrogen Evolution. *RSC Adv.* **2015**, *5* (19), 14074–14080.
- (145) Karjule, N.; Singh, C.; Barrio, J.; Tzadikov, J.; Liberman, I.; Volokh, M.; Palomares, E.; Hod, I.; Shalom, M. Carbon Nitride-Based Photoanode with Enhanced Photostability and Water Oxidation Kinetics. *Adv. Funct. Mater.* **2021**, *31* (25), 2101724.
- (146) Dang, V. D.; Annadurai, T.; Khedulkar, A. P.; Lin, J.-Y.; Adorna, J.; Yu, W.-J.; Pandit, B.; Huynh, T. V.; Doong, R.-A. S-Scheme N-Doped Carbon Dots Anchored g-C<sub>3</sub>N<sub>4</sub>/Fe<sub>2</sub>O<sub>3</sub> Shell/Core Composite for Photoelectrocatalytic Trimethoprim Degradation and Water Splitting. *Appl. Catal. B Environ.* **2023**, *320*, 121928.
- (147) Ragupathi, V.; Raja, M. A.; Panigrahi, P.; Ganapathi Subramaniam, N. CuO/g-C<sub>3</sub>N<sub>4</sub> Nanocomposite as Promising Photocatalyst for Photoelectrochemical Water Splitting. *Optik (Stuttg.)* **2020**, *208*, 164569.
- (148) Serrano-Ruiz, J. C.; Luque, R.; Sepúlveda-Escribano, A. Transformations of Biomass-Derived Platform Molecules: From High



- Added-Value Chemicals to Fuels via Aqueous-Phase Processing. *Chem. Soc. Rev.* **2011**, *40* (11), 5266.
- (149) Sajjadi, B.; Chen, W.-Y.; Raman, A. A. A.; Ibrahim, S. Microalgae Lipid and Biomass for Biofuel Production: A Comprehensive Review on Lipid Enhancement Strategies and Their Effects on Fatty Acid Composition. *Renew. Sustain. Energy Rev.* **2018**, *97*, 200–232.
- (150) Alaswad, A.; Dassisti, M.; Prescott, T.; Olabi, A. G. Technologies and Developments of Third Generation Biofuel Production. *Renew. Sustain. Energy Rev.* **2015**, *51*, 1446–1460.
- (151) Forde, C. J.; Meaney, M.; Carrigan, J. B.; Mills, C.; Boland, S.; Hernon, A. Biobased Fats (Lipids) and Oils from Biomass as a Source of Bioenergy. In *Bioenergy Research: Advances and Applications*; Elsevier, 2014; pp 185–201.
- (152) Sun, Y.; Han, G.; Du, L.; Du, C.; Zhou, X.; Sun, Q.; Gao, Y.; Yin, G.; Li, Y.; Wang, Y. Photoelectrochemistry-Driven Selective Hydroxyl Oxidation of Polyols: Synergy between Au Nanoparticles and C<sub>3</sub>N<sub>4</sub> Nanosheets. *Chem. Catal.* **2021**, *1* (6), 1260–1272.
- (153) Blaskiewicz, S. F.; Santos, H. L. S.; Teixeira, I. F.; Bott-Neto, J. L.; Fernández, P. S.; Mascaro, L. H. Nickel-Modified Polymeric Carbon Nitride for Improving TiO<sub>2</sub>-Based Photoanode: Photoelectrocatalytic Evaluation and Mechanistical Insights. *Mater. Today Nano* **2022**, *18*, 100192.
- (154) Zhao, Y.; Al Abass, N. A.; Malpass-Evans, R.; Carta, M.; McKeown, N. B.; Madrid, E.; Fletcher, P. J.; Marken, F. Photoelectrochemistry of Immobilised Pt@g-C<sub>3</sub>N<sub>4</sub> Mediated by Hydrogen and Enhanced by a Polymer of Intrinsic Microporosity PIM-1. *Electrochem. Commun.* **2019**, *103*, 1–6.
- (155) Githinji, L. J. M.; Musey, M. K.; Ankumah, R. O. Evaluation of the Fate of Ciprofloxacin and Amoxicillin in Domestic Wastewater. *Water, Air, Soil Pollut.* **2011**, *219* (1–4), 191–201.
- (156) Qin, Y.; Yang, S.; You, X.; Liu, Y.; Qin, L.; Li, Y.; Zhang, W.; Liang, W. Carbon Nitride Coupled with Fe-Based MOFs as an Efficient Photoelectrocatalyst for Boosted Degradation of Ciprofloxacin: Mechanism, Pathway and Fate. *Sep. Purif. Technol.* **2022**, *296*, 121325.
- (157) Rafique, N.; Asif, A. H.; Hirani, R. A. K.; Wu, H.; Shi, L.; Zhang, S.; Wang, S.; Yin, Y.; Wang, S.; Sun, H. Versatile Heterojunction of Gold Nanoparticles Modified Phosphorus Doped Carbon Nitride for Enhanced Photo-Electrocatalytic Sensing and Degradation of 4-Chlorophenol. *J. Colloid Interface Sci.* **2023**, *632*, 117–128.
- (158) Xu, H.; Yan, J.; She, X.; Xu, L.; Xia, J.; Xu, Y.; Song, Y.; Huang, L.; Li, H. Graphene-Analogue Carbon Nitride: Novel Exfoliation Synthesis and Its Application in Photocatalysis and Photoelectrochemical Selective Detection of Trace Amount of Cu<sup>2+</sup>. *Nanoscale* **2014**, *6* (3), 1406–1415.
- (159) Wang, P.; Ma, X.; Su, M.; Hao, Q.; Lei, J.; Ju, H. Cathode Photoelectrochemical Sensing of Copper(I) Based on Analyte-Induced Formation of Exciton Trapping. *Chem. Commun.* **2012**, *48* (82), 10216.
- (160) Wang, G.-L.; Xu, J.-J.; Chen, H.-Y. Selective Detection of Trace Amount of Cu<sup>2+</sup> Using Semiconductor Nanoparticles in Photoelectrochemical Analysis. *Nanoscale* **2010**, *2* (7), 1112.
- (161) Xia, P.; Zhu, B.; Yu, J.; Cao, S.; Jaroniec, M. Ultra-Thin Nanosheet Assemblies of Graphitic Carbon Nitride for Enhanced Photocatalytic CO<sub>2</sub> Reduction. *J. Mater. Chem. A* **2017**, *5* (7), 3230–3238.
- (162) Lu, X.; Tan, T. H.; Ng, Y. H.; Amal, R. Highly Selective and Stable Reduction of CO<sub>2</sub> to CO by a Graphitic Carbon Nitride/Carbon Nanotube Composite Electrocatalyst. *Chem. - A Eur. J.* **2016**, *22* (34), 11991–11996.
- (163) Talapaneni, S. N.; Singh, G.; Kim, I. Y.; AlBahily, K.; Al-Muhtaseb, A. H.; Karakoti, A. S.; Tavakkoli, E.; Vinu, A. Nanostructured Carbon Nitrides for CO<sub>2</sub> Capture and Conversion. *Adv. Mater.* **2020**, *32* (18), 1904635.
- (164) Li, Q.; Yang, J.; Feng, D.; Wu, Z.; Wu, Q.; Park, S. S.; Ha, C.-S.; Zhao, D. Facile Synthesis of Porous Carbon Nitride Spheres with Hierarchical Three-Dimensional Mesopores for CO<sub>2</sub> Capture. *Nano Res.* **2010**, *3* (9), 632–642.
- (165) Azofra, L. M.; MacFarlane, D. R.; Sun, C. A DFT Study of Planar vs. Corrugated Graphene-like Carbon Nitride (g-C<sub>3</sub>N<sub>4</sub>) and Its Role in the Catalytic Performance of CO<sub>2</sub> Conversion. *Phys. Chem. Chem. Phys.* **2016**, *18* (27), 18507–18514.
- (166) Zheng, J.; Li, X.; Qin, Y.; Zhang, S.; Sun, M.; Duan, X.; Sun, H.; Li, P.; Wang, S. Zn Phthalocyanine/Carbon Nitride Heterojunction for Visible Light Photoelectrocatalytic Conversion of CO<sub>2</sub> to Methanol. *J. Catal.* **2019**, *371*, 214–223.
- (167) Huang, Z.; Li, F.; Chen, B.; Lu, T.; Yuan, Y.; Yuan, G. Well-Dispersed g-C<sub>3</sub>N<sub>4</sub> Nanophases in Mesoporous Silica Channels and Their Catalytic Activity for Carbon Dioxide Activation and Conversion. *Appl. Catal. B Environ.* **2013**, *136–137*, 269–277.
- (168) Liu, X.; Elgowainy, A.; Wang, M. Life Cycle Energy Use and Greenhouse Gas Emissions of Ammonia Production from Renewable Resources and Industrial By-Products. *Green Chem.* **2020**, *22* (17), 5751–5761.
- (169) Suryanto, B. H. R.; Du, H.-L.; Wang, D.; Chen, J.; Simonov, A. N.; MacFarlane, D. R. Challenges and Prospects in the Catalysis of Electroreduction of Nitrogen to Ammonia. *Nat. Catal.* **2019**, *2* (4), 290–296.
- (170) Chen, Y.; Liu, H.; Ha, N.; Licht, S.; Gu, S.; Li, W. Publisher Correction: Revealing Nitrogen-Containing Species in Commercial Catalysts Used for Ammonia Electrosynthesis. *Nat. Catal.* **2021**, *4* (3), 259–259.
- (171) Andersen, S. Z.; Čolić, V.; Yang, S.; Schwalbe, J. A.; Nielander, A. C.; McEnaney, J. M.; Enemark-Rasmussen, K.; Baker, J. G.; Singh, A. R.; Rohr, B. A.; Statt, M. J.; Blair, S. J.; Mezzavilla, S.; Kibsgaard, J.; Vesborg, P. C. K.; Cargnello, M.; Bent, S. F.; Jaramillo, T. F.; Stephens, I. E. L.; Nørskov, J. K.; Chorkendorff, I. A Rigorous Electrochemical Ammonia Synthesis Protocol with Quantitative Isotope Measurements. *Nature* **2019**, *570* (7762), 504–508.
- (172) Licht, S.; Cui, B.; Wang, B.; Li, F.-F.; Lau, J.; Liu, S. Ammonia Synthesis by N<sub>2</sub> and Steam Electrolysis in Molten Hydroxide Suspensions of Nanoscale Fe<sub>2</sub>O<sub>3</sub>. *Science* (80-). **2014**, *345* (6197), 637–640.
- (173) Liu, Y.; Su, Y.; Quan, X.; Fan, X.; Chen, S.; Yu, H.; Zhao, H.; Zhang, Y.; Zhao, J. Facile Ammonia Synthesis from Electrocatalytic N<sub>2</sub> Reduction under Ambient Conditions on N-Doped Porous Carbon. *ACS Catal.* **2018**, *8* (2), 1186–1191.
- (174) Qin, Q.; Heil, T.; Antonietti, M.; Oschatz, M. Single-Site Gold Catalysts on Hierarchical N-Doped Porous Noble Carbon for Enhanced Electrochemical Reduction of Nitrogen. *Small Methods* **2018**, *2* (12). DOI: 10.1002/smt.201800202.
- (175) Ran, Y.; Yu, X.; Liu, J.; Cui, J.; Wang, J.; Wang, L.; Zhang, Y.; Xiang, X.; Ye, J. Polymeric Carbon Nitride with Frustrated Lewis Pair Sites for Enhanced Photofixation of Nitrogen. *J. Mater. Chem. A* **2020**, *8* (26), 13292–13298.
- (176) Shang, Y.; Zheng, M.; Liu, H.; Jin, X.; Yan, C.; Song, L.; Qi, Z.; Jing, F.; Song, P.; Zhou, X.; Chen, G.; Lv, C. Mimicking Frustrated Lewis Pairs on Graphitic Carbon Nitride for CO<sub>2</sub> Photoreduction. *ACS Catal.* **2023**, *13* (22), 14530–14539.
- (177) Lin, W.; Chen, H.; Lin, G.; Yao, S.; Zhang, Z.; Qi, J.; Jing, M.; Song, W.; Li, J.; Liu, X.; Fu, J.; Dai, S. Creating Frustrated Lewis Pairs in Defective Boron Carbon Nitride for Electrocatalytic Nitrogen Reduction to Ammonia. *Angew. Chem., Int. Ed.* **2022**, *61* (36), e202207807.
- (178) Mushtaq, M. A.; Arif, M.; Fang, X.; Yasin, G.; Ye, W.; Basharat, M.; Zhou, B.; Yang, S.; Ji, S.; Yan, D. Photoelectrochemical Reduction of N<sub>2</sub> to NH<sub>3</sub> under Ambient Conditions through Hierarchical MoSe<sub>2</sub>@g-C<sub>3</sub>N<sub>4</sub> heterojunctions. *J. Mater. Chem. A* **2021**, *9* (5), 2742–2753.
- (179) Galstyan, V.; Comini, E.; Faglia, G.; Sberveglieri, G. Synthesis of Self-Ordered and Well-Aligned Nb<sub>2</sub>O<sub>5</sub> Nanotubes. *CrystEngComm* **2014**, *16* (44), 10273–10279.
- (180) Yang, M.; Zhao, X.; Zheng, S.; Liu, X.; Jin, B.; Li, H.; Gan, Y. A New Electrochemical Platform for Ultrasensitive Detection of

Atrazine Based on Modified Self-Ordered Nb<sub>2</sub>O<sub>5</sub>nanotube Arrays. *J. Electroanal. Chem.* **2017**, *791*, 17–22.

(181) Adán, C.; Marugán, J.; Sánchez, E.; Pablos, C.; Van Grieken, R. Understanding the Effect of Morphology on the Photocatalytic Activity of TiO<sub>2</sub> Nanotube Array Electrodes. *Electrochim. Acta* **2016**, *191*, 521–529.

(182) Lynch, R. P.; Ghicov, A.; Schmuki, P. A Photo-Electrochemical Investigation of Self-Organized TiO<sub>2</sub> Nanotubes. *J. Electrochem. Soc.* **2010**, *157* (3), G76.

(183) Kempken, T.; Hauck, T.; Wang, C.; De Santis, M.; Szulc, W.; Draxler, M.; Sormann, A.; Queipo, P.; Miranda, M.; Croon, D.; et al. *Decarbonisation Pathways 2030 and 2050; Green Steel for Europe Consortium*, 2021.

(184) Babacan, O.; De Causmaecker, S.; Gambhir, A.; Fajardy, M.; Rutherford, A. W.; Fantuzzi, A.; Nelson, J. Assessing the Feasibility of Carbon Dioxide Mitigation Options in Terms of Energy Usage. *Nat. Energy* **2020**, *5* (9), 720–728.

(185) Karjule, N.; Phatake, R. S.; Barzilai, S.; Mondal, B.; Azoulay, A.; Shames, A. I.; Volokh, M.; Alberio, J.; García, H.; Shalom, M. Photoelectrochemical Alcohols Oxidation over Polymeric Carbon Nitride Photoanodes with Simultaneous H<sub>2</sub> Production. *J. Mater. Chem. A* **2022**, *10* (31), 16585–16594.

(186) Su, J.; Zhu, L.; Geng, P.; Chen, G. Self-Assembly Graphitic Carbon Nitride Quantum Dots Anchored on TiO<sub>2</sub> Nanotube Arrays: An Efficient Heterojunction for Pollutants Degradation under Solar Light. *J. Hazard. Mater.* **2016**, *316*, 159–168.

(187) Liang, F.; Zhu, Y. Enhancement of Mineralization Ability for Phenol via Synergetic Effect of Photoelectrocatalysis of G-C<sub>3</sub>N<sub>4</sub> Film. *Appl. Catal. B Environ.* **2016**, *180*, 324–329.

(188) Peng, G.; Qin, J.; Volokh, M.; Shalom, M. Freestanding Hierarchical Carbon Nitride/Carbon-Paper Electrode as a Photoelectrocatalyst for Water Splitting and Dye Degradation. *ACS Appl. Mater. Interfaces* **2019**, *11* (32), 29139–29146.

(189) Shangguan, L.; Yan, C.; Zhang, H.; Xu, G.; Gao, Y.; Li, Y.; Ge, D.; Sun, J. A Visible Light Inducing Photoelectrochemical Biosensor with High-Performance Based on a Porphyrin-Sensitized Carbon Nitride Composite. *New J. Chem.* **2022**, *46* (39), 18680–18687.

(190) Dai, H.; Zhang, S.; Xu, G.; Gong, L.; Fu, M.; Li, X.; Lu, S.; Zeng, C.; Jiang, Y.; Lin, Y.; Chen, G. A Sensitive Arecoline Photoelectrochemical Sensor Based on Graphitic Carbon Nitride Nanosheets Activated by Carbon Nanohorns. *RSC Adv.* **2014**, *4* (22), 11099.

(191) Gouder, A.; Jiménez-Solano, A.; Vargas-Barbosa, N. M.; Podjaski, F.; Lotsch, B. V. Photomemristive Sensing via Charge Storage in 2D Carbon Nitrides. *Mater. Horizons* **2022**, *9* (7), 1866–1877.

(192) Li, R.; Liu, Y.; Cheng, L.; Yang, C.; Zhang, J. Photoelectrochemical Aptasensing of Kanamycin Using Visible Light-Activated Carbon Nitride and Graphene Oxide Nanocomposites. *Anal. Chem.* **2014**, *86* (19), 9372–9375.

(193) Ma, Y.; Fang, Y.; Fu, X.; Wang, X. Photoelectrochemical Conversion of CO<sub>2</sub> into HCOOH Using a Polymeric Carbon Nitride Photoanode and Cu Cathode. *Sustain. Energy Fuels* **2020**, *4* (11), 5812–5817.

(194) Liu, J.; Shi, H.; Shen, Q.; Guo, C.; Zhao, G. A Biomimetic Photoelectrocatalyst of Co-Porphyrin Combined with a g-C<sub>3</sub>N<sub>4</sub> Nanosheet Based on  $\pi$ - $\pi$  Supramolecular Interaction for High-Efficiency CO<sub>2</sub> Reduction in Water Medium. *Green Chem.* **2017**, *19* (24), 5900–5910.

(195) Wang, Q.; Wang, X.; Yu, Z.; Jiang, X.; Chen, J.; Tao, L.; Wang, M.; Shen, Y. Artificial Photosynthesis of Ethanol Using Type-II g-C<sub>3</sub>N<sub>4</sub>/ZnTe Heterojunction in Photoelectrochemical CO<sub>2</sub> Reduction System. *Nano Energy* **2019**, *60*, 827–835.

(196) Alam, K. M.; Chaulagain, N.; Shahini, E.; Masud Rana, M.; Garcia, J.; Kumar, N.; Kobryn, A. E.; Gusarov, S.; Tang, T.; Shankar, K. Low Bandgap Carbon Nitride Nanoparticles Incorporated in Titania Nanotube Arrays by in Situ Electrophoretic Anodization for Photocatalytic CO<sub>2</sub> Reduction. *Chem. Eng. J.* **2023**, *456*, 141067.

(197) Vilanova, A.; Lopes, T.; Mendes, A. Large-Area Photoelectrochemical Water Splitting Using a Multi-Photoelectrode Approach. *J. Power Sources* **2018**, *398*, 224–232.